JACS
JOURNAL OF THE AMERICAN CHEMICAL SOCIETY

Article

pubs.acs.org/JACS

Lewis Base Mediated β-Elimination and Lewis Acid Mediated Insertion Reactions of Disilazido Zirconium Compounds

KaKing Yan, Juan J. Duchimaza Heredia, Arkady Ellern, Mark S. Gordon, and Aaron D. Sadow*

Department of Chemistry, Iowa State University, 1605 Gilman Hall, Ames, Iowa 50011, United States

Supporting Information

ABSTRACT: The reactivity of a series of disilazido zirconocene complexes is dominated by the migration of anionic groups (hydrogen, alkyl, halide, OTf) between the zirconium and silicon centers. The direction of these migrations is controlled by the addition of two-electron donors (Lewis bases) or two-electron acceptors (Lewis acids). The cationic nonclassical $[Cp_2ZrN(SiHMe_2)_2]^+$ ($[\mathbf{2}]^+$) is prepared from $Cp_2Zr\{N(SiHMe_2)_2\}H$ (**1**) and $B(C_6F_5)_3$ or $[Ph_3C][B(C_6F_5)_4]$, while reactions of $B(C_6F_5)_3$ and $Cp_2Zr\{N(SiHMe_2)_2\}R$ (R = Me (**3**), Et (**5**), *n*-C_3H_7 (**7**), CH=CHSiMe$_3$ (**9**)) provide a mixture of $[\mathbf{2}]^+$ and $[Cp_2ZrN(SiHMe_2)(SiRMe_2)]^+$. The latter products are formed through $B(C_6F_5)_3$ abstraction of a β-H and R group migration from Zr to the β-Si center. Related β-hydrogen abstraction and X group migration reactions are observed for $Cp_2Zr\{N(SiHMe_2)_2\}X$ (X = OTf (**11**), Cl (**13**), OMe (**15**), O-*i*-C_3H_7 (**16**)). Alternatively, addition of DMAP (DMAP = 4-(dimethylamino)pyridine) to $[\mathbf{2}]^+$ results in coordination to a Si center and hydrogen migration to zirconium, giving the cationic complex $[Cp_2Zr\{N(SiHMe_2)(SiMe_2DMAP)\}H]^+$ ($[\mathbf{19}]^+$). Related hydrogen migration occurs from $[Cp_2ZrN(SiHMe_2)(SiMe_2OCHMe_2)]^+$ ($[\mathbf{18}]^+$) to give $[Cp_2Zr\{N(SiMe_2DMAP)(SiMe_2OCHMe_2)\}H]^+$ ($[\mathbf{22}]^+$), whereas X group migration is observed upon addition of DMAP to $[Cp_2ZrN(SiHMe_2)(SiMe_2X)]^+$ (X = OTf ($[\mathbf{12}]^+$), Cl ($[\mathbf{14}]^+$)) to give $[Cp_2Zr\{N(SiHMe_2)(SiMe_2DMAP)\}X]^+$ (X = OTf ($[\mathbf{26}]^+$), Cl ($[\mathbf{20}]^+$)). The species involved in these transformations are described by resonance structures that suggest β-elimination. Notably, such pathways are previously unknown in early metal amide chemistry. Finally, these migrations facilitate direct Si−H addition to carbonyls, which is proposed to occur through a pathway that previously had been reserved for later transition metal compounds.

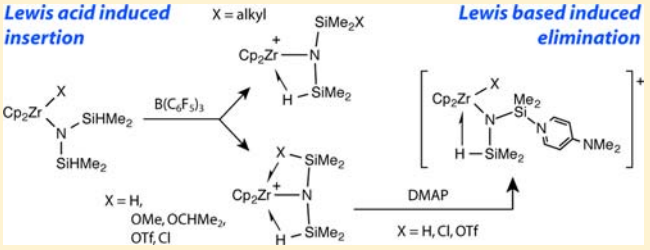

INTRODUCTION

β-elimination and its microscopic reverse, 1,2-migratory insertion, are central to bond-forming and -breaking processes. These reactions are well studied for many metal−ligand pairs; however, the formation of new C−E bonds through insertion reactions into M−E bonds (E = halide, OR, NR_2) remains a major challenge in chemistry. New elementary steps are needed, as these could provide enabling strategies, including catalytic methods, for the efficient synthesis of functionalized organic compounds (e.g., enantioselective hydration, halogenation) or the selective defunctionalization of organic compounds (e.g., for the conversion of biorenewables).

When the migrating group is hydrogen, β-agostic species are the proposed intermediates on this pathway.[1] There have been detailed structural and spectroscopic studies of these compounds, which are suggested to provide a description of the species on the reaction coordinate between the metal alkyl and the metal hydride/olefin.

The bonding nature of agostic interactions, the chemical interpretations offered to describe the interactions, and the anticipated reactions associated with the structures, however, vary with the relative position of a C−H bond with respect to the metal (α, β, etc.), the metal center and its valence, and the other elements present in the agostic ligand.[2] On one end of the continuum, such three-center−two-electron (3c-2e) interactions of aromatic C−H bonds and electron-rich metal centers may be viewed as arrested C−H bond oxidative additions.[3] Similarly, β-agostic organometallics containing a low-valent metal center may be viewed as intermediate between the metal alkyl and a metallacyclopropane hydride resulting from oxidative addition.[4] On the other hand, high-valent metal centers containing β-agostic C−H bonds are characterized as arrested intermediates on the path to an isovalent metal hydride and olefin.[1c,4a,5] β-agostic main-group alkyls are at the other end of the continuum, and electron-density analysis suggests the metal−CH interaction is mainly electrostatic;[4a] β-hydrogen elimination is the least facile in these main-group systems. These electrostatic agostic structures are not established as intermediates on pathways for insertion or elimination.

Thus, β-agostic species have a special relationship with the pathways involving insertion of unsaturated organics into M−H bonds and β-hydrogen elimination. However, strongly Lewis acidic metal centers and polarizable E−E′ bonds (e.g., E−E′ = Si−H, Si−C, B−H) are well-known to form side-on interactions.[2,6−8] These structures are not associated with

Received: August 1, 2013
Published: September 25, 2013

   dx.doi.org/10.1021/ja407950e | J. Am. Chem. Soc. 2013, 135, 15225−15237

insertion/elimination reactions. For example, rare-earth disilazide compounds, such as $[Me_2Si(C_5Me_4)_2]LaN(SiHMe_2)_2$, contain an unusual structure characterized by an obtuse Si−N−Si angle, upfield SiH resonances (2.6−4 ppm) and low $^1J_{SiH}$ values (ca. 130−150 Hz), and low-energy ν_{SiH} bands in the IR spectra (1790−1845 cm^{-1}).[9] The bonding of $[Me_2Si(C_5Me_4)_2]LaN(SiHMe_2)_2$ may be similar to that of the bis(catacolborane) compound $Cp_2Ti(\eta^2\text{-HBcat})_2$, which contains two side-on HBcat ligands,[10] and $Cp_2Zr\{(HB(C_6F_5)_2)_2CH_2\}$, which contains two Zr−H−B bridges.[11]

A key question associated with these bridging structures involves their relationship to the insertion−elimination reactivity. It has been suggested that the rarity of β-eliminations for transition-metal amido compounds[12] is related to the nature of agostic β-CH structures of amide ligands that is distinct in geometry and spectroscopy from the agostic alkyls.[13] For example, β-agostic amides generally feature long N−C bonds, large (ca. 120°) ∠M−N−C angles, and short β-C−H distances,[13] whereas β-agostic alkyls contain short C−C bonds, acute ∠M−C−C angles, and elongated β-C−H bonds.[4b] As the microscopic reverse of β-elimination, the insertion of olefins into more polar M−X bonds (e.g., M−F, M−Cl, M−OR, $M-NR_2$) varies from unknown to rare.[14] Interestingly, a Si−N bond formation was recently described in the reaction of $\{PhC(N\text{-}2,6\text{-}(Me_2HC)_2C_6H_3)_2\}Sc\{N(SiHMe_2)_2\}_2$ and Ph_3C^+, which gives Ph_3CH and $[Sc\{N(SiHMe_2)SiMe_2N(SiHMe_2)_2\}]^+$.[15]

Here, we present a study of the cationic disilazidozirconium compound $[Cp_2ZrN(SiHMe_2)_2]^+$ ($[\mathbf{2}]^+$), which possesses extreme spectroscopic and structural features attributed to the side-on interaction of two SiH groups with a zirconium center. The analogy of the side-on β-Si−H→Zr interaction with agostic β-CH organometallic compounds is supported by pathways to form $[\mathbf{2}]^+$ and its reactivity. This cationic disilazidozirconium reacts with DMAP to give a zirconium hydride through an apparent β-hydrogen elimination process. Addition of the Lewis acid $B(C_6F_5)_3$ to $Cp_2Zr\{N(SiHMe_2)_2\}R$ results in Si−C bond formation through an apparent migratory insertion reaction. In fact, the reactivity of the β-groups on the disilazido ligand, in response to two-electron donors and two-electron acceptors, provides connections to β-elimination and insertion chemistry reminiscent of late transition-metal β-agostic alkyl systems (Scheme 1).

In addition, these compounds react with carbonyls, resulting in hydrosilylation. The mechanism of this hydrosilylation is shown to be related to the hydrogen shuttling between Zr and Si centers. The pathway for this reaction is explored through the study of migration chemistry of β-OR, β-OTf, and β-Cl transfer between zirconium and silicon centers.

Scheme 1. Two-Electron Donor/Acceptor Mediated Anionic Group Transfer

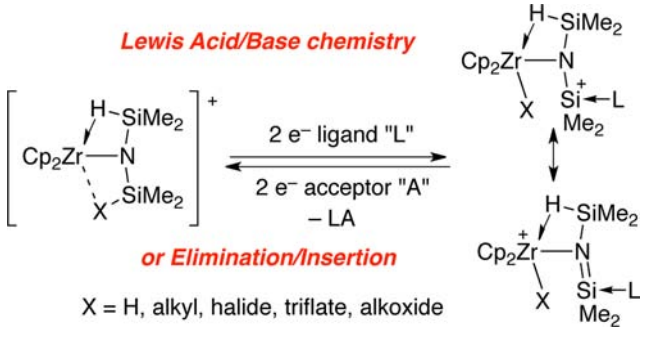

RESULTS

Synthesis and Characterization of the Neutral Precursor of $[Cp_2ZrN(SiHMe_2)_2]^+$. We recently communicated the formation of $Cp_2Zr\{N(SiHMe_2)_2\}H$ (**1**) as a side product in the reaction of $Cp_2Zr\{N(SiHMe_2)_2\}OTf$ and $LiN(SiHMe_2)t\text{-}Bu$.[16] Identification of **1** in that reaction required its independent synthesis, which was achieved by the reaction of Cp_2ZrHCl and $LiN(SiHMe_2)_2$. We have also briefly communicated its solution-phase structure in the context of an unusual γ-abstraction reaction.[17] Surprisingly, $[ZrCl\{N(SiHMe_2)_2\}_2(\mu\text{-Cl})]_2$ is the only other reported zirconium complex containing the $N(SiHMe_2)_2$ moiety,[18] even though this hydrosilazide ligand is widely used in group 3 and lanthanide chemistry,[19] and the related hexamethyldisilazido ligand $[N(SiMe_3)_2]^-$ is important in transition-metal, lanthanide, and main-group chemistry.[20] We describe this compound here because the spectroscopy associated with the nonclassical SiH zirconium interaction represents a starting point for comparison to the unique compounds described here.

The ^1H NMR spectrum of **1** contained the expected resonances, including those for ZrH (5.60 ppm) and SiH (3.78 ppm, $^1J_{SiH}$ = 161.0 Hz). The slightly upfield silicon hydride resonance and moderately low $^1J_{SiH}$ value (cf. $HN(SiHMe_2)_2$, $^1J_{SiH}$ = 170 Hz) suggest a possible side-on Si−H interaction with Zr,[21] however, the $SiMe_2$ groups are equivalent in the ^1H, $^{13}C\{^1H\}$, and ^{29}Si NMR spectra acquired at room temperature.

Therefore, ^1H NMR spectra of **1** in toluene-d_8 were recorded from 298 to 191 K. The SiH and SiMe resonances broaden to the coalescence point at 210 K. At 191 K, the ^1H NMR spectrum contains two SiH resonances and two $SiMe_2$ signals. The two SiH resonances were assigned as nonclassical SiH (2.13 ppm, $^1J_{SiH}$ = 129.7 Hz) and terminal SiH (4.99 ppm, $^1J_{SiH}$ = 179.6 Hz) on the basis of the $^1J_{SiH}$ coupling constants. At 191 K, the ^{29}Si NMR spectrum was resolved to show resonances at −23.1 and −62.9 ppm, which were assigned to silicon atoms with terminal and bridging hydrogens, respectively, by a $^1H-^{29}Si$ HMBC experiment. A similar upfield ^{29}Si NMR resonance was reported for the nonclassical $Cp_2Zr\{N(SiHMe_2)t\text{-}Bu\}H$ (−73.4 ppm),[22] while the downfield signal is comparable to the ^{29}Si NMR resonance of the SiH in $Y\{N(SiHMe_2)_2\}_3(NHC)_2$ (δ −22.5, $^1J_{SiH}$ = 172 Hz; NHC = 1,3-dimethylimidazolin-2-ylidene), which contains short Y−Si distances (Y−Si ≈ 3.13 Å; Y−N−Si = 105.1(3)°) and a low-energy ν_{SiH} (2041 cm^{-1}).[23] Bands at 2047 and 1907 cm^{-1} in the infrared spectrum of **1** further indicate a nonclassical interaction, and IR also provides support for the ZrH group (1559 cm^{-1}).

Interestingly, the reaction of deuterium-labeled Cp_2ZrDCl and $LiN(SiHMe_2)_2$ provides an isotopically scrambled mixture of $Cp_2Zr\{N(SiDMe_2)(SiHMe_2)\}H$ and $Cp_2Zr\{N(SiHMe_2)_2\}D$ (eq 1).

As expected, the deuterium distribution favors its localization in the most tightly bonded position on the basis of IR analysis.[24] Experiments to discern if exchange occurs prior to formation of **1**-d_1 first involved treatment of **1** with D_2 (1 atm) or $PhSiD_3$, with the expectation that ZrH/D_2 and ZrH/SiD exchange would provide $Cp_2Zr\{N(SiHMe_2)_2\}D$. However, these reaction mixtures, heated to 80 °C, give only deuterium-free **1**. Attempts by electrospray MS at determining

dx.doi.org/10.1021/ja407950e | J. Am. Chem. Soc. 2013, 135, 15225−15237

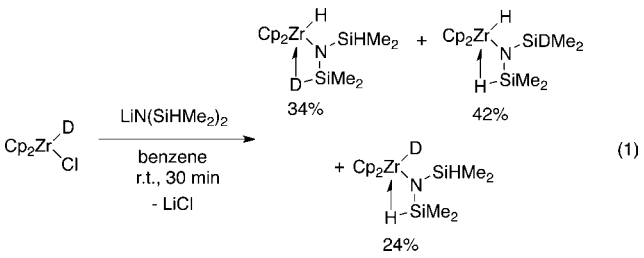

the deuterium distribution (e.g., **1**-d_0, **1**-d_1, **1**-d_2, **1**-d_3) to clarify possible crossover were also unsuccessful. We suspect that H/D exchange between Cp_2ZrDCl and $LiN(SiHMe_2)_2$ occurs prior to Zr−N bond formation because the ZrH and D_2 or $PhSiD_3$ do not exchange under the conditions attempted.

Synthesis of Nonclassical $[Cp_2ZrN(SiHMe_2)_2]^+$. Cationic $[Cp_2ZrN(SiHMe_2)_2]^+$ ($[\mathbf{2}]^+$) is synthesized as the $[HB(C_6F_5)_3]^-$ or $[B(C_6F_5)_4]^-$ salt from reactions of **1** and $B(C_6F_5)_3$ or $[Ph_3C][B(C_6F_5)_4]$ (eq 2). The reactions are

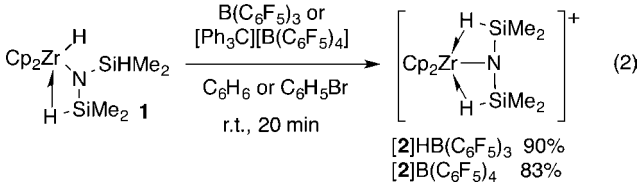

quantitative in bromobenzene-d_5 on a micromolar scale, but benzene is preferable as the solvent in preparatory-scale reactions for easy separation of $[\mathbf{2}]^+$ as an insoluble oil.

The unusual NMR spectroscopic features of the $N(SiHMe_2)_2$ ligand in $[\mathbf{2}]^+$ are similar in both the $[HB(C_6F_5)_3]^-$ and $[B(C_6F_5)_4]^-$ compounds, and the spectroscopic data here are given for the $[B(C_6F_5)_4]^-$ salt.[25] The SiH group in $[\mathbf{2}]^+$ was characterized by a far upfield ^1H NMR signal at −0.48 ppm and an unusually low $^1J_{SiH}$ value (89.3 Hz). For comparison, the ^1H NMR spectrum of the isoelectronic and C_2-symmetric *rac*-$Me_2Si(2\text{-}Me\text{-}Benz\text{-}Ind)_2]YN(SiHMe_2)_2$ contained an upfield SiH signal (2.65 ppm) and a low $^1J_{SiH}$ value (133 Hz).[9] The spectroscopy of $[\mathbf{2}]^+$ is consistent with a C_{2v}-symmetric compound. One ^{29}Si NMR signal was observed at −43 ppm; the ^{29}Si NMR resonance of $[\mathbf{2}]^+$ is upfield of terminal SiH groups in **1** but downfield of the nonclassical SiH group in **1**. In the IR spectrum of $[\mathbf{2}][B(C_6F_5)_4]$, the two bands that are observed at 1738 and 1659 cm^{-1} were assigned to ν_{SiH}. These energies are significantly lower than 2c-2e SiHs in the classical $[Cp_2Zr\{N(SiHMe_2)_2\}OPEt_3]^+$ (2122 cm^{-1}; see below) or the neutral mixed classical/nonclassical **1** (2047 and 1907 cm^{-1}).

X-ray-quality crystals of $[\mathbf{2}][HB(C_6F_5)_3]$ were obtained by slow diffusion of pentane into a concentrated bromobenzene solution at −30 °C (Figure 1). In the solid-state structure, the cationic portion $[Cp_2Zr(N(SiHMe_2)_2]^+$ is separated from the $[HB(C_6F_5)_3]^-$ anion, and the shortest distance in the ion pair is 3.27 Å between an aryl fluoride and one of the silicon centers ($\sum_{SiF}^{VDW}$ = 3.57 Å). The solid-state structure contains a significant, almost perfectly symmetrical distortion of the $N(SiHMe_2)_2$ ligand. The short Zr−Si distances (Zr1−Si1 = 2.8740(8) Å and Zr1−Si2 = 2.8706(7) Å) and the N−Si distances (1.661(2) and 1.662(2) Å) are equivalent within error bounds. For comparison, the Zr−Si distance in the authentic zirconium silyl species $Cp_2ZrSiMe_3(S_2CNEt_2)$ is 2.815(1) Å,[26] while the Zr−Si distance in $Cp_2Zr\{\eta^2\text{-}N(t\text{-}Bu)SiMe_2\}PMe_3$ is 2.654(1) Å.[27] The Si−N distances in $[\mathbf{2}]^+$ are ca. 0.05 Å shorter

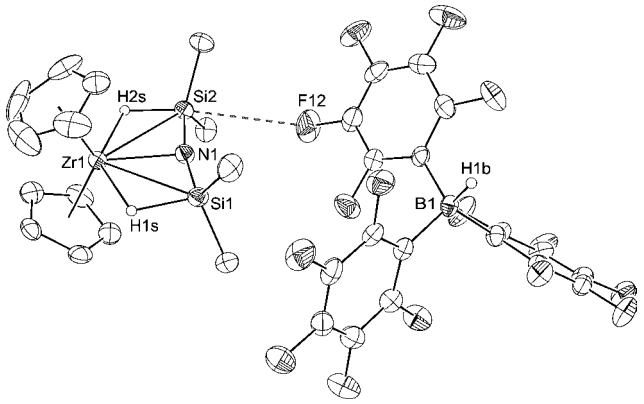

Figure 1. ORTEP diagram of $[Cp_2ZrN(SiHMe_2)_2][HBC_6F_5)_3]$ ($[\mathbf{2}][HB(C_6F_5)_3]$). Ellipsoids are drawn at the 35% probability level. The dashed line between Si2 and F12 indicates the shortest contact between the cation and anion. Significant interatomic distances (Å): Zr1−N1, 2.193(2); Zr1−Si1, 2.8740(8); Zr1−H1s, 2.09(3); Si1−H1s, 1.69(3); Zr1−Si2, 2.8706(7); Zr1−H2s, 2.06(3); Si2−H2s, 1.54(4); N1−Si1, 1.662(2); N1−Si2, 1.661(2). Selected interatomic angles (deg): Zr1−N1−Si1, 95.4(1); Zr1−N1−Si2, 95.3(1); Si1−N1−Si2, 168.9(1); H1s−Zr1−H2s, 137(1); Zr1−N1−Si1−H1s, 0(1); Zr1−N1−Si2−H2s, −3(1), H1si−Si1−Si2−H2s, 3(2).

than the Si−N distance associated with the terminal $SiHMe_2$ in **1** (1.710(2) Å) and ca. 0.02 Å shorter than the Si−N distance of 1.683(2) Å associated with the nonclassical β-$SiHMe_2$ group. The ∠Zr−N−Si angles of $[\mathbf{2}]^+$ are small (95.4(1) and 95.3(1)°), and the ∠Si−N−Si angle approaches linearity at 168.9(2)°.

Interestingly, the Zr−N distance of 2.193(2) Å is 0.05 Å longer than that in **1**. The hydrogen atoms on the $SiHMe_2$ (as well as the H atom in $HB(C_6F_5)_3$ group) were located in the Fourier difference map and refined; the Zr−N bond and the two Si−H bonds are essentially coplanar, as indicated by the torsion angles Zr1−N1−Si1−H1s (0(1)°), Zr1−N1−Si2−H2s (−3(1)°), and H1s−Si1−Si2−H2s (3(2)°).

The Zr1−H1s and Zr1−H2s distances in $[\mathbf{2}]^+$ (2.09(3) and 2.06(3) Å) are long in comparison to the Zr−H distance for the zirconium hydride in **1** (1.90(3) Å), although they are significantly shorter than the Zr−H_{Si} distance of the nonclassical Zr←H−Si in that compound (2.46(4) Å). The terminal Si−H and the nonclassical Si−H distances in **1** are 1.53(4) and 1.47(4) Å, respectively. Furthermore, the $HB(C_6F_5)_3$ counterion has minimal impact on the distances and angles of the $N(SiHMe_2)_2$ ligand. The Zr−H (2.06(3) Å) and Si−H (1.54(4) Å) distances of the $SiHMe_2$ with the fluorine−silicon close contact are within 3× of the esd of the distances in the other $SiHMe_2$ (2.09(3) and 1.69(3) Å, respectively). The observed spectroscopic and structural features provide support for significant nonclassical Zr−$N(SiHMe_2)_2$ interactions in the electron-poor metal complex.[9,19]

Computational Model of $[Cp_2ZrN(SiHMe_2)_2]^+$ ($[\mathbf{2}]^+$). More insight into the relationship between the structural features of $[Cp_2ZrN(SiHMe_2)_2]^+$ ($[\mathbf{2}]^+$) and its spectroscopic properties is provided by a computational study. The geometry optimization and Hessian analysis were carried out using Møller−Plesset second-order perturbation theory (MP2)[28] with a model core potential triple-ζ basis (MCP-TZP)[29] in GAMESS.[30,31] The optimized geometry of the cationic portion of $[Cp_2ZrN(SiHMe_2)_2]^+$ shown in Figure S1 (Supporting Information) is in good agreement with the coordinates

dx.doi.org/10.1021/ja407950e | J. Am. Chem. Soc. 2013, 135, 15225−15237

obtained from an X-ray crystallographic structure determination. For example, the Zr−Si distances, calculated to be 2.861 Å, closely match the experimental Zr−Si distances of 2.8740(8) and 2.8706(7) Å. The calculated Zr−N distance of 2.22 Å is slightly longer than the experimental distance of 2.193(2) Å. The bridging hydrogens are of particular interest, and the calculated Zr−H and Si−H distances are 2.06 and 1.57 Å, respectively.

The vibrational calculation verified that this structure is a minimum on the potential energy surface. Two normal modes are associated with the bridging Zr←H−Si structure; these are symmetric and asymmetric SiH stretching motions with unscaled frequencies of 1800 and 1743 cm^{-1}. These frequencies compare well to the bands in the IR spectrum of $[2]^+$; furthermore, the motion is parallel to the Si−H bond vector rather than along the Zr−H vector.

An orbital localization using the method developed by Edmiston and Ruedenberg[32] reveals two pairs of orbitals of interest (see Figures S2 and S3 in the Supporting Information). One pair of orbitals displays a clear bonding interaction between the three atoms in the Zr−H−Si bridge, while the second pair of orbitals shows a four-atom interaction among Zr, N, and Si. These orbitals suggest the existence of significant interactions between the metal and the silyl groups.

Reactions of $Cp_2Zr\{N(SiHMe_2)_2\}R$ with $B(C_6F_5)_3$. Two pathways that could provide $[2]^+$ from the interaction of **1** and $B(C_6F_5)_3$ are shown in Scheme 2: (A) abstraction of the ZrH

Scheme 2. Possible Pathways for Formation of $[2]^+$: (A) ZrH Abstraction or (B) SiH Abstraction

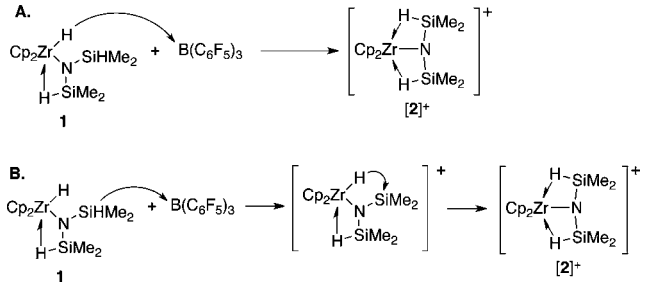

and (B) β-hydrogen abstraction followed by ZrH migration. Although labeled $Cp_2Zr\{N(SiHMe_2)_2\}D$ could potentially resolve this issue, attempted synthesis of **1**-d_1 from Cp_2ZrDCl and $LiN(SiHMe_2)_2$ provides a mixture with $Cp_2Zr\{N(SiHMe_2)_2$-$d_1\}H$ as noted above. Instead, abstraction reactions of alkyl disilazido zirconium compounds were studied to distinguish the abstraction pathways. Furthermore, variation of the alkyl group is a means to control the nucleophilic site in the zirconium compounds, as probed by reactions with $B(C_6F_5)_3$.

Treatment of the zirconium methyl species $Cp_2Zr\{N(SiHMe_2)_2\}Me$ (**3**) with $B(C_6F_5)_3$ gives $[2][MeB(C_6F_5)_3]$ as the major product (70%); however, $[Cp_2ZrN(SiHMe_2)(SiMe_3)][HB(C_6F_5)_3]$ ($[4][HB(C_6F_5)_3]$) is also formed in 30% yield (eq 3). In the reaction mixture, two ^{11}B NMR

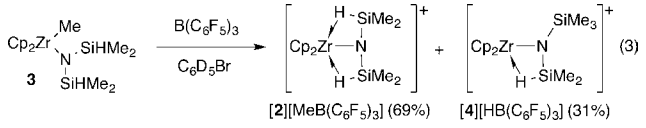

resonances were observed at −14.2 ppm (singlet; major) and −24.8 ppm (doublet, $^1J_{BH}$ = 81.5 Hz; minor). A $^1H-^{11}B$ HMQC experiment contained a cross peak between the resonance at −14.2 ppm and a broad ^1H NMR resonance at 1.11 ppm (3 H) assigned to a $[MeB(C_6F_5)_3]$ group. Integration of the resonances for $[2]^+$ and $[MeB(C_6F_5)_3]$ is the basis for assignment of the major product as $[2][MeB(C_6F_5)_3]$. The minor product $[4][HB(C_6F_5)_3]$, meanwhile, contained a doublet (0.31 ppm, $^3J_{HH}$ = 2.4 Hz, 6 H) and a singlet (0.27 ppm, 9 H) assigned to $SiMe_2$ and $SiMe_3$ groups and a multiplet at 0.64 ppm ($^1J_{SiH}$ = 94.4 Hz) assigned to a nonclassical β-Si−H⇀Zr interaction.

The proposed pathway to the minor product $[4]^+$ involves β-hydrogen abstraction from the disilazido ligand to give a silylium center followed by migration of the methyl from zirconium. On the basis of this idea, zirconium disilazido compounds containing sterically hindered alkyl groups should react with $B(C_6F_5)_3$ more readily by β-hydrogen abstraction than by alkyl group abstraction. Competition experiments were designed to test this, and the compounds $Cp_2Zr\{N(SiHMe_2)_2\}R$ (R = Et (**5**), n-C_3H_7 (**7**), CH═CHSiMe$_3$ (**9**)) were allowed to react with $B(C_6F_5)_3$ to give mixtures of $[2]^+$ and $[Cp_2ZrN(SiHMe_2)(SiRMe_2)]^+$ (R = Et (**6**), n-C_3H_7 (**8**), CH═CHSiMe$_3$ (**10**)) (Scheme 3). Importantly, the ratio of $[Cp_2ZrN(SiHMe_2)(SiRMe_2)]^+$ to $[2]^+$ increases as the alkyl group is varied, following the trend Me < Et < n-C_3H_7 < CH═CHSiMe$_3$.

Scheme 3. Competition between [Zr]R Abstraction and β-Hydrogen Abstraction in Reactions of Mixed Alkyl Disilazido Zirconium Compounds and $B(C_6F_5)_3$

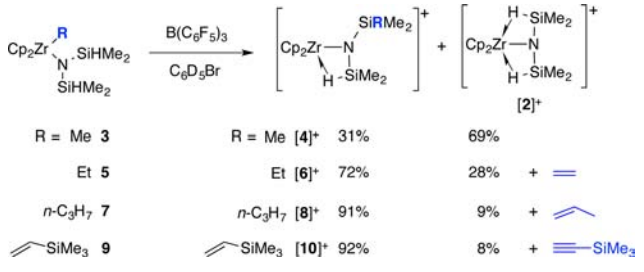

Although $[4]^+$, $[6]^+$, $[8]^+$, and $[10]^+$ could not be separated from the side product $[2]^+$, the assignments of Si−C bond formation are unambiguously supported by $^1H-^{29}Si$ HMBC and COSY experiments. For example, in compound $[10]^+$, a cross peak is detected between the ^{29}Si NMR signal at −12.9 ppm and the ^1H NMR vinylic signals at 6.43 and 6.75 ppm.

Interestingly, $[HB(C_6F_5)_3]^-$ is the only counterion in the reaction mixture resulting from interaction of $B(C_6F_5)_3$ and the ethyl, n-propyl, and trimethylsilylvinyl zirconium compounds. Meanwhile, ethylene, propylene, and trimethylsilylacetylene are formed as byproducts, and these data are consistent with β-H abstraction from the alkyl group. Thus, β-hydrogen abstraction (as part of either SiH or CH groups) is favored with respect to alkyl group abstraction.[33] Previously, we observed a concentration dependence on β-hydrogen abstraction vs alkyl group abstraction in reactions of ZnR_2 and bis(4,4-dimethyl-2-oxazolinyl)phenylborane.[34] However, in the current system carbon−boron bond formation is below ^1H and ^{11}B NMR detection limits, and the product ratios are similar in reactions performed at concentrations from 2.4 to 9.6 mM.

Reactions of $Cp_2Zr\{N(SiHMe_2)_2\}X$ with $B(C_6F_5)_3$. Zirconium alkyls, and likely a zirconium hydride, migrate to the β-silicon center of the silazido ligand upon addition of Lewis

dx.doi.org/10.1021/ja407950e | J. Am. Chem. Soc. 2013, 135, 15225−15237

acids. Therefore, we were interested in studying the migration of other anionic groups, such as OR, Cl, and OTf.

The compounds $Cp_2Zr\{N(SiHMe_2)_2\}X$ (X = OTf (**11**), Cl (**13**), OMe (**15**), $OCHMe_2$ (**16**)) react with $B(C_6F_5)_3$ or $[Ph_3C][B(C_6F_5)_4]$ in benzene to give $[Cp_2ZrN(SiHMe_2)(SiMe_2\text{-}\mu\text{-}X)]^+$ (X = OTf ($[\mathbf{12}]^+$), Cl ($[\mathbf{14}]^+$), OMe ($[\mathbf{17}]^+$), $OCHMe_2$ ($[\mathbf{18}]^+$)) (Scheme 4).

Scheme 4. β-Hydrogen Abstraction Reactions of Zirconium Disilazido Triflate, Chloride, and Alkoxide Compounds

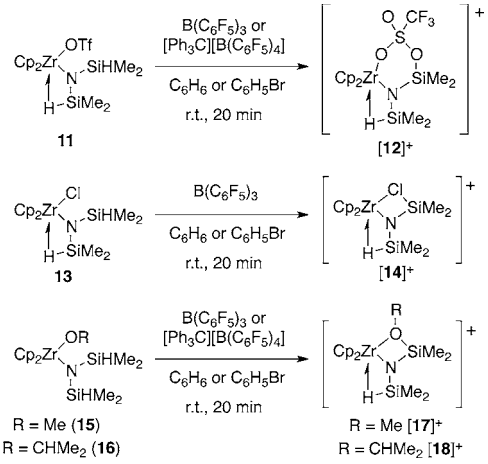

In all cases, hydrogen abstraction is supported by the formation of $[HB(C_6F_5)_3]^-$ (e.g., $[\mathbf{12}][HB(C_6F_5)_3]$: ^{11}B NMR −24.8 ppm, $^1J_{BH}$ = 87.1 Hz) or Ph_3CH. The series of products $[\mathbf{12}]^+$, $[\mathbf{14}]^+$, $[\mathbf{17}]^+$, and $[\mathbf{18}]^+$ contain similar spectroscopic features for the $N(SiHMe_2)(SiMe_2X)$ ligand. The cationic $[Cp_2ZrN(SiHMe_2)(SiMe_2X)]^+$ is C_s symmetric, as two $SiMe_2$ and one C_5H_5 resonance were observed in the ^1H NMR spectrum. All the compounds feature upfield-shifted ^1H NMR resonances for the β-SiH, extremely low $^1J_{SiH}$ values, and ^{29}Si NMR resonances for the β-SiH group ranging from −26 to −32 ppm (Table 1). These assignments are supported by $^1H-^{29}Si$ HMBC experiments.

The upfield SiH chemical shifts and $^1J_{SiH}$ values for both salts of $[\mathbf{12}]^+$ provide support for the nonclassical structure. The ^{29}Si NMR resonances at 21.4 ppm ($SiMe_2OTf$) and −25.9 ppm ($SiHMe_2$) were assigned by $^1H-^{29}Si$ HMBC experiments. For comparison, the Me_3SiOTf ^{29}Si NMR chemical shift is +43.5 ppm and the $Me(Et_2N)_2SiOTf$ ^{29}Si NMR chemical shift is −19 ppm.[35]

X-ray-quality crystals of $[\mathbf{12}][HB(C_6F_5)_3]$ were obtained from a concentrated bromobenzene solution layered with pentane cooled to −30 °C. A single-crystal X-ray diffraction study shows the OTf^- is bridging between Zr and a β-Si center (Figure 2). In addition, there is a short Zr1−Si2 distance of

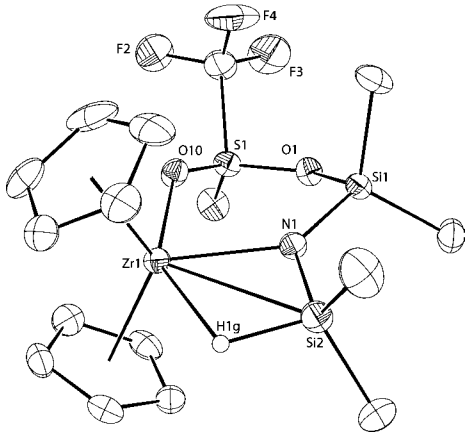

Figure 2. ORTEP diagram of $[Cp_2ZrN(SiHMe_2)(SiMe_2\text{-}\mu\text{-}\kappa^2\text{-}OTf)][HB(C_6F_5)_3]$ ($[\mathbf{12}][HB(C_6F_5)_3]$) with ellipsoids plotted at the 35% probability level. The cationic portion of the structure is illustrated, and only the bridging hydrogen atom is plotted. All other hydrogen atoms, the $HB(C_6F_5)_3$ counterion, and a disordered C_6H_5Br molecule are not included for clarity.

2.890(1) Å. The Zr1−H1g distance of 2.20(3) Å for the nonclassical SiH is between the related distances in neutral **1** and cationic $[\mathbf{2}]^+$. However, $[\mathbf{12}]^+$ does not display the other unusual structural features of $[\mathbf{2}]^+$; namely, the Si1−N1−Si2 angle is normal (127.7(2)°) and the Zr1−Si1 distance is long (3.59 Å).

The Zr1−O10 distance of 2.313(2) Å is slightly longer than the Zr−OTf distance in $[Cp_2Zr(\kappa^1\text{-}OTf)(\mu\text{-}H)]_2$ (2.205(2)

Table 1. ^1H and ^{29}Si NMR Data of Cationic β-SiH Containing Dihydrodisilazido Zirconium Compounds

compd[a]	Si*H* (ppm)	$^1J_{SiH}$ (Hz)	*Si*HMe_2 (ppm)	*Si*Me_2X (ppm)
$[Cp_2ZrN(SiHMe_2)_2][HB(C_6F_5)_3]$ ($[\mathbf{2}][HB(CF_5)_3]$)	−0.44	107	−42.7	n.a.
$[Cp_2ZrN(SiHMe_2)_2][B(C_6F_5)_4]$ ($[\mathbf{2}][B(C_6F_5)_4]$)	−0.48	89	−43.7	n.a.
$[Cp_2ZrN(SiHMe_2)(SiMe_3)]^+$ ($[\mathbf{4}]^+$)	0.64	94	8.2	−0.2
$[Cp_2ZrN(SiHMe_2)(SiMe_2Et)]^+$ ($[\mathbf{6}]^+$)	0.5	94	7.4	5.6
$[Cp_2ZrN(SiHMe_2)(SiMe_2\text{-}n\text{-}C_3H_7)]^+$ ($[\mathbf{8}]^+$)	0.46	87	5.2	6.0
$[Cp_2ZrN(SiHMe_2)(SiMe_2CHCHSiMe_3)]^+$ ($[\mathbf{10}]^+$)	0.56	89	−11.5	−5.2
$[Cp_2ZrN(SiHMe_2)(SiMe_2\text{-}\mu\text{-}\kappa^2\text{-}OTf)][HB(C_6F_5)_3]$ ($[\mathbf{12}][HB(C_6F_5)_3]$)	0.22	107	−25.9	21.4
$[\mathbf{12}][B(C_6F_5)_4]$	0.18	99	−25.2	21.4
$[Cp_2ZrN(SiHMe_2)(SiMe_2\text{-}\mu\text{-}Cl)]^+$ ($[\mathbf{14}]^+$)	0.65	89	−32.5	29.6
$[Cp_2ZrN(SiHMe_2)(SiMe_2\text{-}\mu\text{-}OMe)]^+$ ($[\mathbf{17}]^+$)	0.34	96	−29.7	20.4
$[Cp_2ZrN(SiHMe_2)(SiMe_2\text{-}\mu\text{-}OCHMe_2)]^+$ $[\mathbf{18}]^+$	0.41	94	−33.0	13.2
$[Cp_2Zr\{N(SiHMe_2)(SiMe_2DMAP)\}H]^+$ ($[\mathbf{19}]^+$)	0.95	118[b]	−63.6	−0.6
$[Cp_2Zr\{N(SiHMe_2)(SiMe_2DMAP)\}Cl]^+$ ($[\mathbf{20}]^+$)	3.04	155	−34.2	5.7
$[Cp_2Zr\{N(SiHMe_2)(SiMe_2py)\}OTf]^+$ ($[\mathbf{25}]^+$)	1.27	115	−24.0	14.4
$[Cp_2Zr\{N(SiHMe_2)(SiMe_2DMAP)\}OTf]^+$ ($[\mathbf{26}]^+$)	1.37	115	−26.6	7.7
$[Cp_2Zr\{N(SiHMe_2)(SiMe_2OPEt_3)\}OTf]^+$ ($[\mathbf{27}]^+$)	1.35	115	−29.1	2.4

[a]All compounds are $[HB(C_6F_5)_3]$ salts unless otherwise noted. [b]Acquired at −88 °C.

dx.doi.org/10.1021/ja407950e | J. Am. Chem. Soc. 2013, 135, 15225−15237

Å).[36] The Si1−O1 distance of 1.788(2) Å is within the sum of covalent radii.[37] These distances, the ^{29}Si NMR chemical shift of the SiOTf center, and the short Zr−H and Zr−Si distances argue for greater positive charge localization on Zr rather than on the Si center.

Similarly, the reaction of $Cp_2Zr\{N(SiHMe_2)_2\}Cl$ and $B(C_6F_5)_3$ gives $[Cp_2ZrN(SiHMe_2)(SiMe_2$-μ-$Cl)]^+$ ([**14**][HB-$(C_6F_5)_3$]) via β-hydrogen abstraction. The ^{29}Si NMR chemical shift for the $SiMe_2Cl$ moiety is 29.6 ppm; for comparison, the value for Me_3SiCl is 30.2 ppm[38] and the value for Me_2NSiMe_2Cl is 13.9 ppm.[39]

Finally, reactions of **1** and paraformaldehyde or acetone provide the alkoxide (disilazido)zirconium compounds $Cp_2Zr\{N(SiHMe_2)_2\}OR$ (R = Me (**15**), $CHMe_2$ (**16**)). Notably, reactions of **1** and excess ketone or aldehyde do not result in insertion into the Si−H bonds of the $N(SiHMe_2)_2$ group under these conditions (see reactions of $[\mathbf{2}]^+$ and carbonyls below for such transformations). The bonding of the $N(SiHMe_2)_2$ group in neutral $Cp_2Zr\{N(SiHMe_2)_2\}OR$ is classical, as evidenced by downfield SiH chemical shifts (δ 4.71 and 4.77), high SiH coupling constants ($^1J_{SiH}$ = 180 and 182 Hz), and high-energy ν_{SiH} bands (**15**, 2078 cm^{-1}; **16**, 2113 and 2051 cm^{-1}). The structure is further supported by a single-crystal X-ray diffraction study of **16** (see the Supporting Information). The ∠Zr1−N1−Si1 and ∠Zr1−N1−Si2 angles are 121.4(1) and 122.2(1)°, respectively; the Zr1−Si1 and Zr1−Si2 distances are 3.3714(9) and 3.3824(8) Å. In addition, the Zr1−O1 distance is 1.937(2) Å while the O1−Si1 distance is 3.353(2) Å.

The reaction of methoxyzirconium species **15** and $B(C_6F_5)_3$ or $[Ph_3C][B(C_6F_5)_4]$ provides $[Cp_2ZrN(SiHMe_2)(SiMe_2$-μ-OMe)]$^+$ ($[\mathbf{17}]^+$). Likewise, the reaction of isopropoxyzirconium species **16** and $B(C_6F_5)_3$ or $[Ph_3C][B(C_6F_5)_4]$ yields ($[\mathbf{18}]^+$) (Scheme 4). Compounds $[\mathbf{17}]^+$ and $[\mathbf{18}]^+$, remarkably, also feature spectroscopic features associated with nonclassical Zr←H−Si structures. This, perhaps, is most notable because the neutral precursors **15** and **16** contain only 2c-2e SiH moieties. Abstraction of a β-hydrogen and formation of a Zr−O−Si bridging interaction might be expected to geometrically limit possible Zr←H−Si interactions. Instead, the structure of $[Cp_2ZrN(SiMe_2OCHMe_2)_2]^+$ suggests that the N-$(SiMe_2OCHMe_2)$ moiety is best described as a β-silyl ether, and this permits a long Zr−O distance (see below).

Overall, the addition of Lewis acids to $Cp_2Zr\{N(SiHMe_2)_2\}$-X-type compounds results in β-hydrogen abstraction and Si−X bond formation, accompanied by the formation of nonclassical Zr←H−Si structures.

Reactions with Lewis Bases and Hydride Migration. Remarkably, the cationic disilazide compounds $[\mathbf{2}][HB(C_6F_5)_3]$ and $[\mathbf{2}][B(C_6F_5)_4]$ react with 4-(dimethylamino)-pyridine (DMAP) to give $[Cp_2Zr\{N(SiHMe_2)$-$(SiMe_2DMAP)\}H]^+$ ($[\mathbf{19}]^+$; X = $HB(C_6F_5)_3$, $B(C_6F_5)_4$) (eq 4); the product contains only one β−Si−H⇀Zr group and a new zirconium hydride.

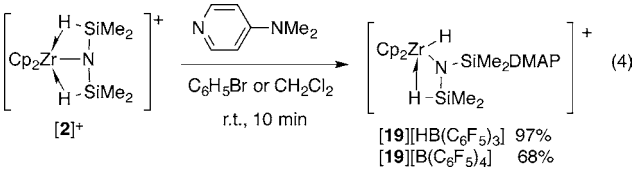

A ^{1}H NMR spectrum of $[\mathbf{19}]^+$ acquired at room temperature in methylene chloride-d_2 was slightly broad, but the $SiMe_2$ (0.51 and 0.21 ppm), ZrH (4.43 ppm), SiH (1.27 ppm), and aromatic (pyridine) CH resonances (7.93 and 6.78 ppm) were readily assigned (all assignments are supported by COSY experiments, chemical shift, and integration). The resonances assigned to C_5H_5 (5.81 ppm) and NMe_2 (3.21 ppm) were sharp. However, we were unable to detect ^{29}Si NMR resonances at room temperature using ^{29}Si INEPT experiments.

The low-temperature NMR spectra of $[\mathbf{19}]^+$ were sharper and better resolved. At 185 K, two ^{29}Si resonances were observed at −0.5 and −63.6 ppm. Only the signal at −63.6 ppm ($^1J_{SiH}$ = 118 Hz) was observed in a ^{29}Si INEPT experiment optimized for J_{SiH} = 120 Hz, and the signal at −0.5 ppm was only detected in a ^{29}Si INEPT experiment optimized for long-range proton coupling (J_{SiH} = 7 Hz). In a ^{1}H−^{29}Si HMBC experiment optimized for long-range ^{1}H−^{29}Si coupling (J_{SiH} = 7 Hz) shown in Figure 3, the −63.6 ppm ^{29}Si resonance was

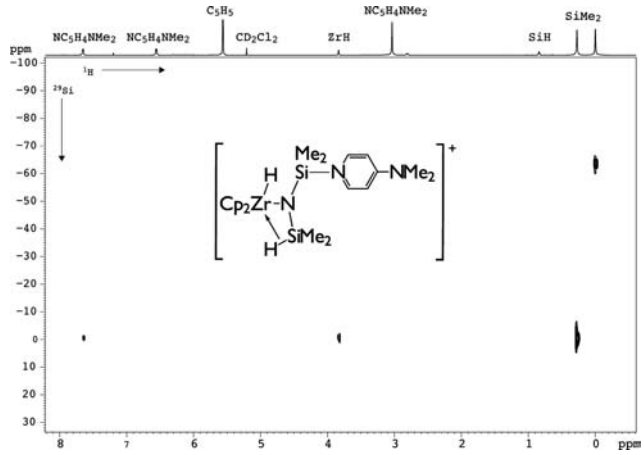

Figure 3. ^{1}H−^{29}Si HMBC experiment on $[Cp_2Zr\{N(SiHMe_2)$-$(SiMe_2DMAP)\}H][HB(C_6F_5)_3]$ ($[\mathbf{19}][HB(C_6F_5)_3]$) in methylene chloride-$d_2$ optimized for J_{SiH} = 7 Hz and acquired at 185 K. The experiment is optimized for long-range bonding; thus, there is no cross peak for the SiH and the cross peak between Zr*H* and *Si*Me_2DMAP shows small scalar coupling.

correlated with a ^{1}H NMR signal at 0.21 ppm assigned to $SiMe_2$. In that experiment, cross peaks from the ^{29}Si signal at −0.5 ppm were correlated in the ^{1}H dimension to the second $SiMe_2$ group (0.51 ppm), the signal at 3.95 ppm assigned to the ZrH, and the aromatic resonances assigned to DMAP (7.93 ppm). The correlations between the silicon atom and the aromatic signals provide convincing evidence that DMAP is coordinated to silicon rather than zirconium.

Further evidence for Si−N bond formation is provided by a ^{1}H−^{15}N HMBC experiment, which showed a correlation between the pyridine nitrogen and the $SiMe_2$ at 0.51 ppm. We assign the ^{1}H NMR signal at 3.95 ppm to a zirconium hydride on the basis of a correlation in a COSY experiment between that signal and the resonance at 0.95 ppm assigned to β-Si−H⇀Zr. The extent of interaction between the ZrH and the silicon center in the $SiMe_2DMAP$ group is considerably less than that in $[\mathbf{2}]^+$ ($^1J_{SiH}$ = 89 Hz). The chemical shift of 3.95 ppm is upfield relative to the signal for the zirconium hydride in **1** (5.60 ppm). However, zirconium hydrides have been assigned to signals as upfield as 3.12 ppm in $Cp_2Zr(H)NH_2BH_3$.[40] Although spectra were obtained for $[\mathbf{19}]^+$ in methylene chloride-d_2, after solutions are heated to 120 °C for 45 min in that solvent, a reaction occurs to provide $[Cp_2Zr\{N$-

dx.doi.org/10.1021/ja407950e | J. Am. Chem. Soc. 2013, 135, 15225−15237

$(SiMe_2DMAP)(SiHMe_2)\}Cl]^+$ ($[\mathbf{20}]^+$). The identity of $[\mathbf{20}]^+$ is supported by its independent synthesis (see below).

The broad, room-temperature ^1H NMR spectrum for compound $[\mathbf{19}]^+$ suggests a slow exchange process involving the silyl groups, the zirconium hydride, and DMAP. In an EXSY experiment performed at room temperature, a cross peak between the $SiMe_2$ and $SiHMe_2$ groups and a cross peak between ZrH and SiH showed exchange involving hydrogen transfer between Zr and both silicon centers. The coalescence temperature for this exchange process is above room temperature and has not been observed, and the process also slows down at low temperature. The EXSY experiment indicates that migration of hydrogen from silicon to zirconium is reversible. Despite this, the reactivity of $[\mathbf{19}]^+$, such as its conversion to $[\mathbf{20}]^+$ and a cyclometalation described later, occur without apparent loss of DMAP.

In contrast to the chemistry with DMAP, reactions of $[\mathbf{2}]^+$ and Et_3PO afford $[Cp_2Zr\{N(SiHMe_2)_2\}OPEt_3]^+$ ($[\mathbf{21}]^+$; eq 5).

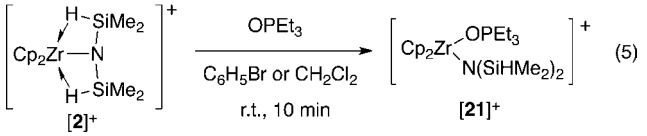

(5)

The structure of $[\mathbf{21}]^+$ is readily distinguished from that of the DMAP adduct $[\mathbf{19}]^+$ by NMR spectroscopy. In the ^1H NMR spectrum of $[\mathbf{21}]^+$, a single resonance assigned to equivalent SiMe groups was observed at 0.11 ppm ($^3J_{HH}$ = 4.2 Hz; 12 H), and a signal at 4.09 ppm ($^1J_{SiH}$ = 181.8 Hz; 2 H) was assigned as a SiH on the basis of its correlation to the $SiMe_2$ signal in a COSY experiment. The typical chemical shift and $^1J_{SiH}$ values suggest that $[\mathbf{21}]^+$ contains terminal silicon hydride groups. A single ^{29}Si NMR signal was detected at −19.2 ppm. In addition, compound $[\mathbf{19}]^+$ and $OPEt_3$ react to give $[\mathbf{21}]^+$ and free DMAP, while starting materials are observed in the reaction of $[\mathbf{21}]^+$ and DMAP.

On the basis of the interesting results in reactions of $[\mathbf{2}]^+$ with two-electron donors, we also examined reactions of $[\mathbf{18}]^+$ with coordinating ligands. The reaction of $[\mathbf{18}]^+$ with DMAP in CH_2Cl_2 forms $[Cp_2Zr\{N(SiMe_2OCHMe_2)(SiMe_2DMAP)\}H]^+$ ($[\mathbf{22}]^+$; Scheme 5).

Scheme 5. Reversible Hydrogen Migration between Zr and Si Controlled by the Addition or Removal of a Two-Electron Donor

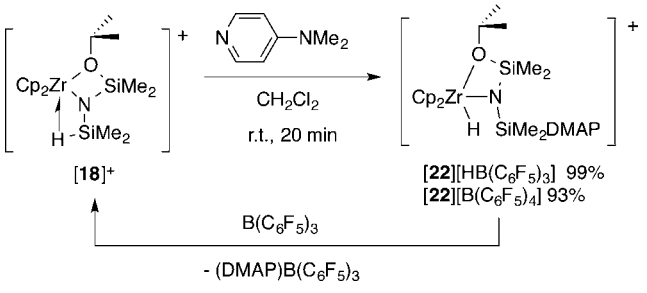

In contrast to the NMR spectroscopy of $[\mathbf{19}]^+$, the ^1H, ^{13}C, and ^{29}Si NMR spectra of $[\mathbf{22}]^+$ were sharp at room temperature. The ^1H NMR resonances of ZrH, $SiMe_2DMAP$, and $SiMe_2OCHMe_2$ of $[\mathbf{22}][HB(C_6F_5)_3]$ were observed at 4.44 (1 H), 0.39 (6 H), and −0.06 ppm (6 H), respectively. The ZrH signal at 4.44 ppm did not show any correlation to either $SiMe_2$ signal in COSY experiments. Two ^{29}Si NMR resonances were detected at 16.6 and −11.0 ppm with INEPT experiments. $^1H-^{29}Si$ HMBC experiments (optimized for J_{SiH} = 7 Hz) contained cross peaks between the ^{29}Si signal at 16.6 ppm and the resonances assigned to one $SiMe_2$ group, $OCHMe_2$, and ZrH; the upfield ^{29}Si resonance (−11.0 ppm) showed long-range correlations to the other $SiMe_2$ group, ZrH, and the α-CH protons of DMAP. The last cross peak supports the structural assignment involving a DMAP−silicon interaction. Moreover, the long-range correlations between the Zr−H proton and *both* Si atoms ($SiMe_2DMAP$ and $SiMe_2OCHMe_2$) in the $^1H-^{29}Si$ HMBC experiment provide support for a Zr−H group that is formed via DMAP-induced hydrogen elimination.

Interestingly, this migration is chemically reversible. Addition of $B(C_6F_5)_3$ to a methylene chloride solution of $[\mathbf{22}][HB(C_6F_5)_3]$ provides $[\mathbf{18}][HB(C_6F_5)_3]$ and $(DMAP)B(C_6F_5)_3$. Furthermore, compound $[\mathbf{22}]^+$ reacts similarly to related zirconium hydride **1**, as well as $Cp_2Zr\{N(SiMe_3)_2\}H$, by undergoing γ-hydrogen abstraction.[17,41] Thus, thermolysis of $[\mathbf{22}]^+$ in a sealed glass tube at 140 °C for 4 h affords H_2 and $[Cp_2ZrN(SiMe_2OCHMe_2)SiMe(DMAP)CH_2]^+$ ($[\mathbf{23}]^+$; eq 6).

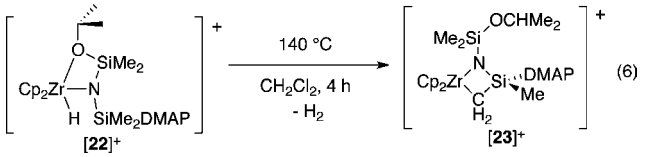

(6)

The ^1H NMR spectrum of $[\mathbf{23}]^+$ contained signals assigned to a diastereotopic isopropyl group (1.32 ppm, $^3J_{HH}$ = 6.1 Hz; 1.29 ppm, $^3J_{HH}$ = 6.1 Hz) and a diastereotopic $ZrCH_2$ group (1.14 ppm, $^2J_{HH}$ = 13.4 Hz; 0.95 ppm, $^2J_{HH}$ = 13.3 Hz), as well as three SiMe signals (0.44, 0.17, and 0.14 ppm). A $^1H-^{29}Si$ HMBC experiment revealed correlations from the stereogenic Si center to the aromatic α-CH proton of DMAP and the diastereotopic CH_2, which unambiguously confirms the connectivity between $ZrCH_2Si$ and DMAP.

As in the reaction of $[\mathbf{2}]^+$ and $OPEt_3$, phosphine oxide coordinates to the zirconium center in $[\mathbf{18}]^+$ to give $[Cp_2Zr\{N(SiHMe_2)(SiMe_2OCHMe_2)\}OPEt_3]^+$ ($[\mathbf{24}]^+$; eq 7).

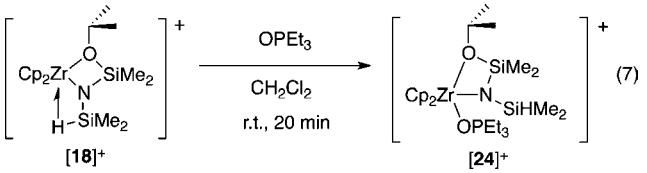

(7)

The NMR spectroscopy of $[\mathbf{24}]^+$, particularly the SiH group (δ 4.04, $^1J_{SiH}$ = 187 Hz), distinguishes its connectivity from that of the silicon-coordinated DMAP species $[\mathbf{22}]^+$. In a COSY experiment, the ^1H NMR resonance at 0.12 ppm (6 H) assigned to the $SiMe_2$ correlated with the SiH resonance at 4.04 ppm. Two ^{29}Si resonances were detected in ^{29}Si INEPT and $^1H-^{29}Si$ HMBC experiments at −5.1 and −21.9 ppm. In the latter experiments, cross peaks between the ^{29}Si resonance at −5.1 ppm and the methine proton (3.74 ppm) of the $OCHMe_2$ group and $OSiMe_2$ protons (0.06 ppm, 6 H) provided evidence for an Si−O−C linkage in the $SiOCHMe_2$ moiety.

Halide and Pseudohalide Migration. Reactions of the nonclassical SiH and bridging triflate compound $[\mathbf{12}]^+$ with pyridine, DMAP, or $OPEt_3$ induce migration of OTf^- to zirconium to provide the series of compounds $[Cp_2Zr\{N-$

dx.doi.org/10.1021/ja407950e | J. Am. Chem. Soc. 2013, 135, 15225−15237

$(SiHMe_2)(SiMe_2L\}OTf]^+$ (L = py ([**25**]$^+$), DMAP ([**26**]$^+$), $OPEt_3$ ([**27**]$^+$); eq 8). The β-hydrogen does not migrate, and the nonclassical Zr←H−Si structure is evident in the products.

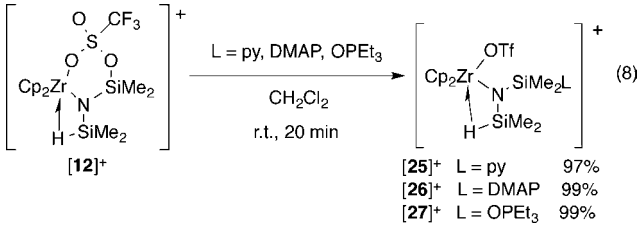

(8)

The ^{1}H NMR spectra of [**25**]$^+$−[**27**]$^+$ contain resonances in the region 1.27−1.37 ppm assigned to SiH groups; the upfield chemical shift and the $^1J_{SiH}$ values of 115 Hz establish the nonclassical Zr←H−Si structures. ^{1}H−^{29}Si HMBC experiments revealed two silicon signals for [**25**]$^+$−[**27**]$^+$; correlations between the further downfield signals and aromatic resonances of pyridine and DMAP established Si−L bond formation. These correlations are not available for $OPEt_3$, and in that case we relied on the similarity in other spectral features of [**27**]$^+$ with those of [**25**]$^+$ and [**26**]$^+$. The upfield ^{29}Si NMR resonances correlated in ^{1}H−^{29}Si HMBC experiments to the upfield ^{1}H NMR peaks assigned to the SiH in [**25**]$^+$−[**27**]$^+$. The ^{19}F NMR chemical shifts of the signals assigned to OTf^- for compounds [**25**]$^+$−[**27**] varied only 0.3 ppm from −78.5 to −78.8 ppm, whereas the signal for bridging OTf^- in [**12**]$^+$ appears at −75.0 ppm. The monodentate OTf^- in **11** is −78.2 ppm. Thus, of three possible outcomes that include coordination to zirconium, coordination to silicon with hydrogen migration, and coordination to silicon with OTf^- migration, the observed products are consistent with the last pathway.

Likewise, reaction of chloride-bridged [**14**]$^+$ and DMAP gives $Cp_2Zr\{N(SiHMe_2)(SiMe_2DMAP)\}Cl]^+$ ([**20**]$^+$). As mentioned above, [**20**]$^+$ is also prepared quantitatively through the thermolysis of [**19**]$^+$ in methylene chloride. Similarly, the reaction of [**19**]$^+$ and MeOTf gives [**26**]$^+$ and methane.

Hydrosilylation of Carbonyls for the Synthesis of Cationic $[Cp_2ZrN(SiMe_2OR)_2]^+$. The implications of the nonclassical structure of [**2**]$^+$ on reactivity was further explored with carbonyl reagents. Compound [**2**]$^+$ and 2 equiv of paraformaldehyde react at 80 °C in bromobenzene to yield $[Cp_2ZrN(SiMe_2OMe)_2]^+$ ([**28**]$^+$; eq 9).

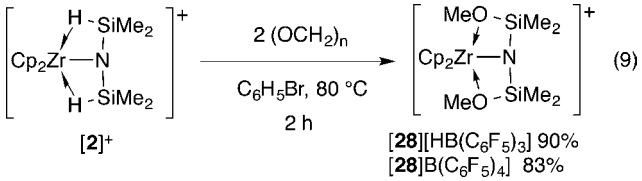

(9)

In the ^{1}H NMR spectrum of [**28**]$^+$, a resonance at 2.99 ppm (6 H) in the ^{1}H NMR spectrum is characteristic of a methoxy group. The observed single ^{29}Si NMR signal at 9.6 ppm was >50 ppm farther downfield than the corresponding resonance at −43 ppm in the starting material [**2**]$^+$. The formation of a SiOMe group was unambiguously supported by a ^{1}H−^{29}Si HMBC experiment that contained a cross peak between the methoxy group and the silicon center. The methoxy group, however, is likely bridging silicon and zirconium, as shown below in the structure of $[Cp_2ZrN(SiMe_2OCHMe_2)_2]^+$.

The preparation of [**28**]$^+$ requires elevated temperature to dissolve and depolymerize paraformaldehyde. In contrast, the reaction of [**2**]$^+$ and 2 equiv of acetone occurs within 10 min at room temperature in bromobenzene or methylene chloride to give $[Cp_2ZrN(SiMe_2OCHMe_2)_2]^+$ ([**29**]$^+$) (Scheme 6).

Scheme 6. Hydrosilylation of Acetone by [2]$^+$ Followed by a Slower Hydroboration with $HB(C_6F_5)_3^-$

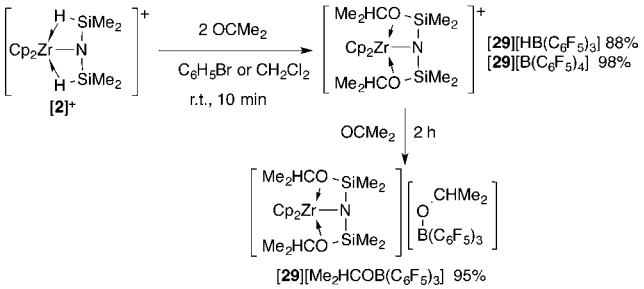

The ^{1}H NMR spectrum of [**29**]$^+$ contained a multiplet at 4.14 ppm (2 H) and a doublet at 1.51 ppm ($^3J_{HH}$ = 6.5 Hz, 12 H) that are characteristic of the isopropoxy group. One ^{29}Si resonance was detected by ^{29}Si INEPT experiments at 5.2 ppm, and this signal correlated to ^{1}H NMR signals of $SiMe_2$ (12 H) and OC*H*Me_2 in ^{1}H−^{29}Si HMBC experiments. Thus, the spectroscopy unambiguously identified the $SiOCHMe_2$ moiety.

X-ray-quality crystals of [**29**][$HB(C_6F_5)_3$] are obtained from a concentrated methylene chloride solution cooled to −30 °C (Figure 4). Hydrosilylation of the acetone is confirmed, and the resulting isopropoxy groups bridge between the silicon and zirconium centers. The Zr1−O1 and Zr1−O2 distances of 2.385(4) and 2.333(3) Å are similar to other distances in three-coordinated oxygen centers bonded to silicon and zirconium

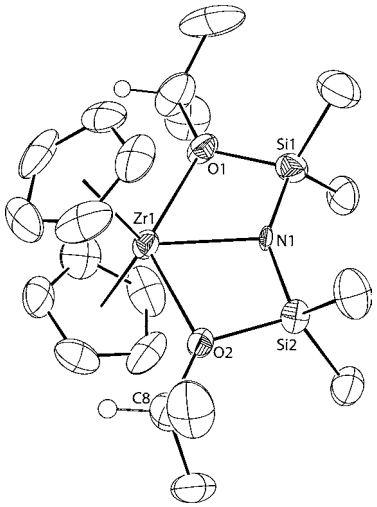

Figure 4. ORTEP diagram of the cationic portion of [**29**]$^+$ with ellipsoids plotted at the 50% probability level. $HB(C_6F_5)_3$ and a CH_2Cl_2 solvent molecule are not illustrated, nor are the hydrogens on the C_5H_5 and methyl groups. Significant interatomic distances (Å): Zr1−N1, 2.121(4); Zr1−O1, 2.385(4); Zr1−O2, 2.333(3); N1−Si1, 1.642(4); N1−Si2, 1.712(4); Si1−O1, 1.711(4); Si2−O2, 1.699(4). Selected interatomic angles (deg): Zr1−N1−Si1, 108.5(2); Zr1−N1−Si2, 104.88(19); Si1−N1−Si2, 146.6(2); O1−Zr1−O2, 130.7(1); Zr1−N1−Si1−O1, −1.4(2); Zr1−N1−Si2−O2, −2.3(2), O1−Si1−Si2−O2, −4.0(2).

dx.doi.org/10.1021/ja407950e | J. Am. Chem. Soc. 2013, 135, 15225−15237

where the O center is unambiguously described as an L-type ligand,[42] such as $\{(C_6H_{11}NSiMe_2)_2O\}Zr(CH_2Ph)_2$, which features a Zr−O distance of 2.381(2) Å.[43] The Si1−O1 and Si2−O2 distances of 1.711(4) and 1.699(4) Å are slightly longer than the other distances in that compound. For comparison, the Zr−O distance in neutral $Cp_2Zr\{N(SiHMe_2)_2\}OCHMe_2$ is 1.937(2) Å, while the Zr−O and Si−O distances in $Cp_2Zr(OSiMe_2CH_2Cl)Cl$ are 1.943(3) and 1.609(3) Å, respectively.[44] On the basis of these structural comparisons, $[\mathbf{29}]^+$ is probably best described as a $N(SiMe_2OCHMe_2)_2$ tridentate L_2X-type ligand coordinated to the Zr center through an amide and two silyl ether groups.

Addition of excess acetone (>3 equiv) to $[\mathbf{2}][HB(C_6F_5)_3]$ yields $[Cp_2ZrN(SiMe_2OCHMe_2)_2][(Me_2HCOB(C_6F_5)_3]$ ($[\mathbf{29}][Me_2HCOB(C_6F_5)_3]$) over 2 h (Scheme 6). The formation of $[\mathbf{29}][HB(C_6F_5)_3]$ as an intermediate occurs within 5 min, followed by slow conversion of $[HB(C_6F_5)_3]$ into $[Me_2HCOB(C_6F_5)_3]^-$. The ^{1}H NMR spectrum of $[\mathbf{29}]$-$[Me_2HCOB(C_6F_5)_3]$ contained two sets of isopropoxy resonances in a 2:1 ratio assigned to Me_2HCOSi (1.51 ppm, $^3J_{HH}$ = 6.5 Hz; 4.14 ppm) and Me_2HCOB (0.88 ppm, $^3J_{HH}$ = 5.9 Hz; 3.60 ppm). Furthermore, the resonance in the ^{11}B NMR spectrum at −3.4 ppm is characteristic of formation of an alkoxyborate moiety.[45] Interestingly, the rate of insertion involving the nonclassical SiH group (10 min) is much faster than that involving the BH (2 h). Furthermore, conversion of $[HB(C_6F_5)_3]$ in $[\mathbf{29}]^+$ into the $[Me_2HCOB(C_6F_5)_3]$ anion is not detected in the absence of excess acetone.

DISCUSSION

Migrations from Zr to Si. The migration of an anionic group (H, alkyl, halide, triflate, alkoxide) from zirconium to a β-silicon center can be described as an X group abstraction by a transient cationic β-silylium electrophile generated through hydrogen abstraction by a Lewis acid. This description is based on a resonance structure of the transient where charge is localized on the silicon center (Scheme 7, structure I.A.). Additionally, silylium cations are known as strong Lewis acids in hydride and halide abstractions.[46−48]

Scheme 7. Comparisons of (I) Borane-Induced X Group Migration through a Silanimine, (II) β-Hydrogen Abstraction To Generate Transient E=SiR$_2$, and (III) Insertion of an Olefin into a M−C Bond

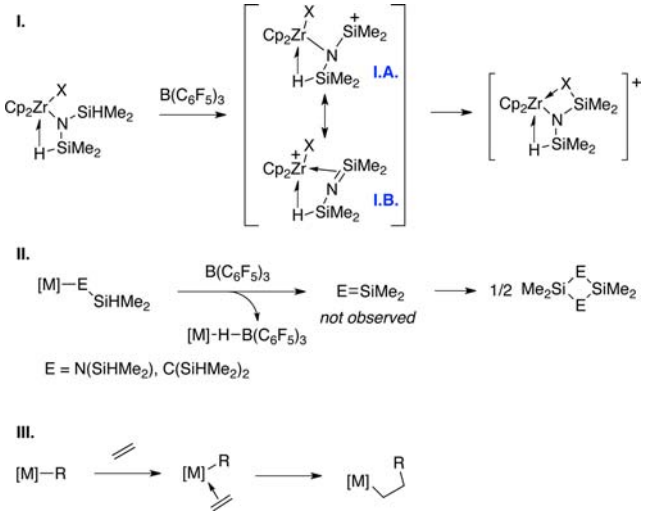

An alternative resonance structure of the cationic transient shows localization of charge on the electropositive Zr center, in which case the intermediate is described as a cationic zirconium-coordinated silanimine complex (Scheme 7, structure I.B.). Support for this description is provided by reactions of β-SiH containing alkyl moieties $MC(SiHMe_2)_3$ and $B(C_6F_5)_3$, which produce $M-H-B(C_6F_5)_3$ and disilacyclobutane (Scheme 7, part II).[49]

The latter species is postulated to form via $2\pi + 2\pi$ cyclodimerization of the silene intermediate that forms upon β-hydrogen abstraction. Further support for this description is given by abstraction of a β-hydrogen from an alkyl ligand in $Cp_2Zr\{N(SiHMe_2)_2\}R$ that provides the olefin, as noted above. Finally, the intermediacy of a coordinated $Me_2Si{=}NSiHMe_2$ in the present system is supported by the selective dimerization observed in the absence of a reactive M−X group.

Both 1,1-insertions and 1,2-insertions are better described as migrations of an X-type ligand to an electrophilic, metal-coordinated carbon center (Scheme 7, part III), as evidenced by stereochemical studies of insertion reactions.[50,51] Thus, formation of Si−X bonds from the polarized silanimine/silylium functionality in $[Cp_2Zr\{N(SiMe_2)(SiHMe_2)\}X]^+$ is best understood with both resonance structures (I.A. and I.B.) that highlight polarization of unsaturated moieties as an important component of insertion reactions.

The influence of the alkyl group R on reactions of $Cp_2Zr\{N(SiHMe_2)_2\}R$ and Lewis acids provides data to compare the interpretation of abstraction. In these reactions, four pathways may be postulated on the basis of structures of the products: (a) alkyl group abstraction by the Lewis acid, (b) β-hydrogen abstraction from the alkyl group, (c) β-hydrogen abstraction from the disilazido group followed by β-hydrogen abstraction by the transient silylium electrophile, and (d) β-hydrogen abstraction from the disilazido group followed by alkyl group migration (Scheme 8).

Scheme 8. Possible Pathways for the Interaction of $Cp_2Zr\{N(SiHMe_2)_2\}R$ and $B(C_6F_5)_3$

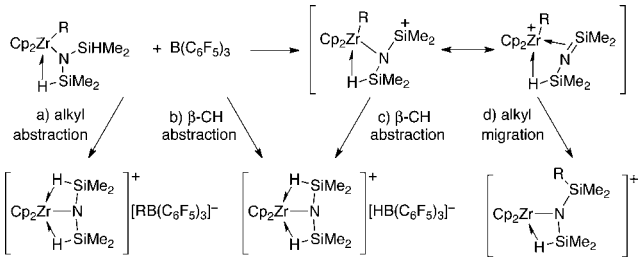

With larger R groups (e.g., n-C_3H_7) the pathway that provides Si−C bond formation (alkyl migration) is the most favored, and alkyl group abstraction products (pathway a) are not detected. A minor amount of β-CH abstraction (pathways b and c) is evident by the formation of $[\mathbf{2}]^+$ and the corresponding olefin. It is important that alkyl group migration is favored over β-CH abstraction. The dominance of alkyl migration suggests that the silanimine resonance structure is a more important contributor than the silylium structure in Scheme 8; the latter would be expected to react by β-hydrogen abstraction because the well-defined Lewis acid $B(C_6F_5)_3$ reacts by β-hydrogen abstraction in this system. Furthermore, the much larger concentration of charge at Zr than at Si that is inferred by experiment is supported by the MP2 calculations of

dx.doi.org/10.1021/ja407950e | J. Am. Chem. Soc. 2013, 135, 15225−15237

$[Cp_2ZrN(SiHMe_2)_2]^+$. The latter predict an order of magnitude larger positive charge on Zr (1.77) than on Si (0.19), on the basis of Mulliken populations.

A related X group migration was also observed for $Cp_2Zr\{N(SiHMe_2)_2\}X$ and $B(C_6F_5)_3$, where X is chloride, triflate, methoxide, and isopropoxide. In the final products, bridging Zr−X−Si structures are obtained (compounds $[\mathbf{12}]^+$, $[\mathbf{14}]^+$, $[\mathbf{17}]^+$, and $[\mathbf{18}]^+$, respectively). In these bridging compounds, the X group on $X-SiMe_2$ behaves as a L-type, two-electron donor to the electron-deficient Zr center. This assignment is supported by ^{29}Si NMR spectroscopy and X-ray diffraction studies of $[\mathbf{29}]^+$.

In addition, a recent report documents a related $N(SiHMe_2)_2$ migration from a scandium center to a β-Si upon addition of a Lewis acid, and a similar sequential hydrogen abstraction/silazide migration sequence was proposed.[15] These similarities indicate that the reactivity pattern described in the current contribution is not simply limited to the Cp_2Zr system.

Migrations from Si to Zr. The entry points to the Si to Zr migration chemistry in all cases are bridging Si−X−Zr structures. DMAP induces migration of a monovalent group from silicon to the zirconium center. The migrating group may be hydrogen, chloride, or triflate. In the systems in which both β-H and β-X (X = Cl, OTf) are present, migration of X rather than H is observed, whereas competition between β-H and β-OR results in hydrogen migration. Other nucleophilic ligands coordinate, such as $OPEt_3$ and pyridine, and the binding site varies between Si and Zr depending on the identity of the migrating X group. There are similarities in these donor-assisted migrations to β-elimination as well as to Lewis base induced cleavage reactions. The comparison between β-elimination and Lewis acid/base chemistry is evaluated through analogies to main-group and transition-metal chemistry and through analysis of the microscopic reverse reaction.

A related Lewis base induced hydride transfer is reported for the reaction of the symmetrical hydrogen-bridged, cationic disilyl species $[(\mu\text{-H})(Me_2Si(CH_2)_3SiMe_2]^+$ and acetonitrile that gives $[(Me_2HSi(CH_2)_3SiMe_2(NCMe)]^+$.[48]

In contrast to the $[Si-H-Si]^+$ system, the atoms in the bridging Zr←H−Si moieties are inequivalent. In these structures, a coordinating ligand may interact with the zirconium center or the silicon center and disrupt the M−H−Si interaction. These bridging structures, and their interactions with ligands, may also be compared to M−H−BR_n adducts, which are known for rare-earth-metal, main-group-metal, and transition-metal complexes. In rare-earth examples, $Cp^*_2LaHBEt_3$[52] and $(C_5H_4CMe_3)_2SmHBEt_3$[53] are coordinated by THF without displacing the Ln−H−B interaction, whereas $(C_5H_3(CMe_3)_2)_2CeHBPh_3$ spontaneously dissociates BPh_3.[54] In Zr−H−BR_n compounds, it has been pointed out that Zr−H or B−H cleavage may result, either spontaneously or through the assistance of a donor such as Et_2O.[55] The main-group compound $KHB(C_6F_5)_3$ reacts with TMEDA to give $(tmeda)KHB(C_6F_5)_3$,[56] whereas $(C_5(SiMe_3)_3H_2)CaHBEt_3$ is inert to PMe_3.[57] Thus, the cleavage site of the M−H−B bridging interaction depends on M and substituents on the boron center.

Alternatively, rare-earth-metal tetraalkylaluminate adducts react with pyridine to form metal alkyls.[58,59] Although aluminum−pyridine adducts are formed in these reactions, both a [M]−Me bond and an [Al]−Me bond are broken during the transformation; in addition, both bridging methyl groups are engaged in electron-deficient bonding, and therefore elimination gives saturated products (as opposed to unsaturated products). While $[Cp_2ZrMe_2AlMe_2]^+$ is proposed to dissociate $AlMe_3$ to generate active $[Cp_2ZrMe]^+$ catalytic species, the only donors present in such polymerizations are olefins.[60] Additionally, a yttrium hydridoaluminate is converted to a $[Y(\mu\text{-H})]_2$ species in the presence of excess DIBAH.[61] That conversion occurs without an additional two-electron donor. However, it should also be noted that the nucleophilicity of a hydrosilane is proposed to be enhanced by coordination of a Lewis base such as F^-, for example, to facilitate the hydrosilylation of a carbonyl compound.[62] This analogy may extend to the Lewis base-facilitated hydrogen transfer to an electrophilic Zr center.

Thus, the present example of DMAP coordination to the β-silicon of the disilazido ligand is distinguished from typical Lewis base chemistry of bridging aluminates or borates. Despite the strong nonclassical interactions, it should be noted that β-hydrogen elimination in transition-metal amido compounds is rare,[12] and β-eliminations of amides from d^0 transition-metal and rare-earth-metal centers are unknown. Still, there are similarities in the present system to the β-elimination chemistry of transition-metal alkyls.[4a]

The unsaturated β-elimination products from reactions of low-valent transition-metal alkyls are stabilized by two-electron π back-donation to give metallacyclopropyl resonance structures. In the cationic zirconium disilazido compounds, two electrons from DMAP serve as a surrogate for metal-based π back-donation to stabilize the silanimine (Scheme 9).

Scheme 9. Comparison of H Migration Products in (A) DMAP-Induced Reactions and (B) Low-Valent β-Eliminations

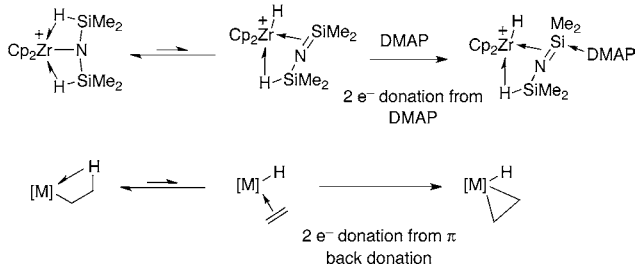

β-hydrogen elimination and insertion into a M−H bond are related by the principle of microscopic reversibility. Likewise, this Si to Zr migration and its microscopic reverse of Zr to Si migrations are controlled by the addition of Lewis acids or Lewis bases. Thus, the zirconium hydride DMAP adduct $[\mathbf{22}]^+$ and $B(C_6F_5)_3$ react to re-form β-SiH-containing $[\mathbf{18}]^+$ and $(DMAP)B(C_6F_5)_3$.

The migration of halide and triflate from Si to Zr should also be considered in the context of abstraction vs elimination. While the lone-pair electrons on X argue for the Lewis acid model, several other comparisons are worth noting. First, β-Cl eliminations from metal chloroalkyls limit vinyl chloride polymerizations.[63] Moreover, similar β-X elimination reactions were observed from $Cp^*_2ScCH_2CH_2X$ (X = PPh_2, OEt, F).[64] In these systems, as well as in the current cationic zirconium compounds, β-X elimination products are formed instead of β-H, at least as the isolated products.

Finally, it is remarkable that the nonclassical Zr←H−Si moiety in $[\mathbf{2}]^+$ behaves as if it is an intermediate on the reaction coordinate for β-hydrogen elimination. This comparison further reinforces the description of the reaction as a Lewis base

dx.doi.org/10.1021/ja407950e | J. Am. Chem. Soc. 2013, 135, 15225−15237

mediated β-hydrogen elimination and highlights the similarities between these bridging SiH groups and β-agostic alkyls.

Carbonyl Hydrosilylation. Given the observations of hydrogen migration between silicon and zirconium centers, several pathways for the formation of silyl ethers from the carbonyl compounds may be considered. First (pathway A), a carbonyl oxygen may coordinate to the zirconium center, disrupting the nonclassical Zr←H−Si structure, as was observed in the interaction of $[\mathbf{2}]^+$ and $OPEt_3$. Transfer of hydrogen to the carbonyl carbon, followed by alkoxide migration to silicon, would then provide the hydrosilylated product. Alternatively (pathway B), the carbonyl may coordinate to the silicon center to induce migration of hydrogen from silicon to form a ZrH group, which subsequently is transferred to the carbon of the coordinated carbonyl. A third possible mechanism (pathway C) again invokes carbonyl-assisted ZrH formation which is then followed by insertion of a second carbonyl into the Zr−H bond to give a zirconium alkoxide. Dissociation of the coordinated carbonyl from the silicon center, followed by migration of the alkoxide to silicon, would then provide the product. In general, Lewis acid assisted hydrosilylation reactions involve hydrogen abstraction from silane, coordination of the carbonyl oxygen to a silylium center, and transfer of hydride from silicon to the resulting carbocation.[65] Note that the cationic components of complexes containing $[HB(C_6F_5)_3]^-$ or $[B(C_6F_5)_4]^-$ react similarly, and the hydroboration of the carbonyls by $[HB(C_6F_5)_3]$ is slow relative to the hydrosilylation. These observations rule out a $B(C_6F_5)_3$-catalyzed process and hydride transfer from $[HB(C_6F_5)_3]^-$, as proposed by Piers (not shown in Scheme 10).[47]

Scheme 10. Possible Pathways for the Hydrosilylation of Carbonyl Compounds by $[\mathbf{2}]^+$

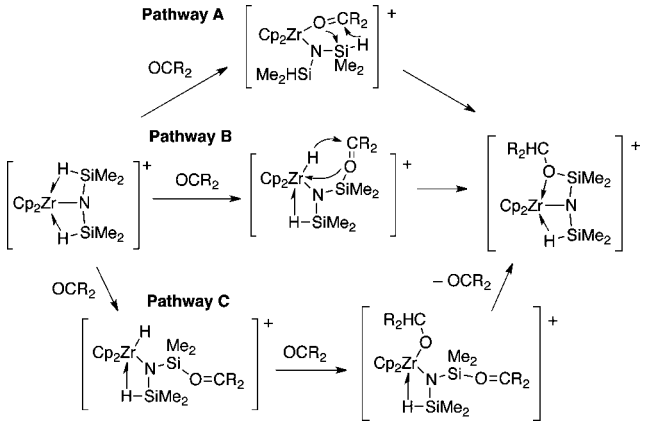

Attempts to distinguish these pathways through kinetic studies were not successful, because the reaction of $[\mathbf{2}]^+$ and acetone is finished before it can be measured even at 200 K. Furthermore, kinetic studies were limited by the heterogeneous nature of the reaction between $[\mathbf{2}]^+$ and paraformaldehyde. Other carbonyl compounds, including bulky aldehydes and ketones, also were not useful for kinetic studies.

Thus, alternative tests are needed to probe the pathway(s) by which hydrosilylation occurs. While the Zr−H group in **1** reacts with acetone and paraformaldehyde to form **15** and **16**, the β-SiH groups in these molecules do not react with either substrate (at least under the conditions tested). We then attempted to block the zirconium center by $OPEt_3$ coordination. In fact, reactions of the $OPEt_3$ adduct $[Cp_2Zr\{N(SiHMe_2)_2\}OPEt_3]^+$ ($[\mathbf{21}]^+$) with paraformaldehyde or acetone provided the hydrosilylation products, albeit qualitatively more slowly than in the absence of $OPEt_3$. Still, $OPEt_3$ is displaced from zirconium in the final product.

Similarly, reactions of DMAP adduct $[\mathbf{19}]^+$ and paraformaldehyde provide $[\mathbf{28}]^+$. Again, these reactions are slower than the corresponding reaction of $[\mathbf{2}]^+$ and the carbonyls, suggesting that the silicon site is involved in the hydrosilylation pathway. Interestingly, the additional product $[Cp_2ZrN(SiMe_2OCMeCH_2)_2]^+$ and H_2 are obtained (from reactions of DMAP adduct $[\mathbf{19}]^+$ and acetone); these products correspond to deprotonation of acetone and formation of an enolate (the ratio of enolate to insertion is 1.8:1). Enolate formation is not observed in reactions of $[\mathbf{2}]^+$ and acetone or in reactions of $OPEt_3$ adduct $[Cp_2Zr\{N(SiHMe_2)_2\}OPEt_3]^+$ and acetone. This observation suggests that the ZrH can react with acetone through two routes, insertion or deprotonation/enolate formation. Because enolate formation is not observed in reactions of $[\mathbf{2}]^+$, it seems unlikely that pathway C is dominant.

These experiments suggest that both sites are necessary for the hydrosilylation. In accordance with this idea, compounds $[\mathbf{25}]^+$−$[\mathbf{27}]^+$, which contain OTf bonded to the zirconium center, a Lewis base coordinated to a silicon center, and a nonclassical β-SiH are unchanged in the presence of acetone, even at elevated temperature (85 °C). In those compounds, excess DMAP does not induce migration of hydrogen to zirconium.

Pathway A should be available for compounds such as $[\mathbf{25}]^+$ that feature a nonclassical Zr←H−Si structure that could be disrupted by carbonyl coordination to zirconium. However, no hydrosilylation is observed with $[\mathbf{25}]^+$, and thus we rule out pathway A. Furthermore, the $OPEt_3$ adduct $[\mathbf{21}]^+$, as a model for the intermediate on pathway A, features classical 2c-2e SiH moieties that should not be reactive in hydrosilylation.[47] Although coordination of a carbonyl to a Lewis acid Mo center was recently proposed as a pathway for hydrosilylation on the basis of an isotopic labeling experiment,[66] this mechanism seems unlikely in the current case.

Instead, a pathway in which hydride migrates to zirconium is favored, as suggested by pathways B and C. The formation of enolates from the cationic ZrH DMAP adduct $[\mathbf{19}]^+$ suggests that pathway C should also feature enolate formation in general. Because $[\mathbf{2}]^+$ and acetone react to give enolate-free products, we rule out pathway C for the hydrosilylation of carbonyls by $[\mathbf{2}]^+$.

The remaining mechanism, pathway B, features formation of a Si−O bond and Zr−H bond, followed by hydrogen transfer to the electrophilic carbonyl site. The proposed pathway is similar to that proposed by Abu-Omar and co-workers for the Re(V)-catalyzed hydrosilylation of carbonyls, on the basis of elimination of a mechanism involving carbonyl insertion into a Re^V−H bond.[67] A related proposed mechanism is described by Brookhart that features an Ir^{III}−(η^1-H-SiR_3) group that transfers R_3Si^+ to the carbonyl oxygen.[68] Notably, the zirconium center in $[\mathbf{2}]^+$ is d^0 and thus π back-donation is not available to stabilize the M−(η^2-$HSiR_3$) interaction or to populate the σ^* orbital to assist in the Si−H bond cleavage.

CONCLUSION

The nonclassical Zr←H−Si group in compounds $[\mathbf{2}]^+$ and its derivatives provide a connection between the insertion/β-agostic CH/elimination organometallic reaction pathways and inorganic Lewis acid/Lewis base chemistry of silylium, boranes,

dx.doi.org/10.1021/ja407950e | J. Am. Chem. Soc. 2013, 135, 15225−15237

and trialkylaluminum/tetraalkylaluminate adducts. This comparison is important, particularly with respect to the transfer of anionic hydride and alkyl ligands between Lewis acidic centers. Furthermore, the addition of a two-electron donor to facilitate hydrogen migration shows the connection between the two seemingly unrelated organometallic systems in terms of reactivity. The transformation from a nonclassical Zr←H−Si group to a trapped β-eliminated product is noteworthy.

In addition, the nonclassical structures in $[\mathbf{2}]^+$ are central to the observed carbonyl hydrosilylation reaction. Here, it is seen that the nonclassical structure facilitates the overall addition reaction without generating an enolate side product, as is observed with the cationic zirconium hydride $[\mathbf{19}]^+$. The similarities between the chemistry of $[\mathbf{2}]^+$ and the proposed catalytic mechanisms based on Re^V and Ir^{III} catalysts further support the generality of the nonclassical pathway across the transition-metal series.

Finally, it is worth considering that the tetramethyldisilazido ligand used here is commonly employed in f-element chemistry, as well as in group 2 chemistry. The amine $HN(SiHMe_2)_2$ is relatively acidic,[9] and relatively inert compounds are often obtained. Although the precursors and $LnMN(SiHMe_2)_2$ compounds are more easily handled than corresponding alkyls, they often do not provide direct access to catalytically active species. The Lewis acid/Lewis base treatment strategy developed here provides an effective route for the synthesis of catalytically reactive hydrides from stable precursors.

■ ASSOCIATED CONTENT

Supporting Information

Text, tables, and CIF files giving experimental procedures, crystallographic data, and computational details. This material is available free of charge via the Internet at http://pubs.acs.org.

■ AUTHOR INFORMATION

Corresponding Author

sadow@iastate.edu

Notes

The authors declare no competing financial interest.

■ ACKNOWLEDGMENTS

A.D.S. and K.Y. gratefully thank the National Science Foundation (CHE-0955635 and MRI-1040098) for financial support. J.J.D.H. and M.S.G. acknowledge support from National Science Foundation grant CHE-1147446 and an AGEP supplement to that grant.

■ REFERENCES

(1) (a) Schmidt, G. F.; Brookhart, M. *J. Am. Chem. Soc.* **1985**, *107*, 1443−1444. (b) Doherty, N. M.; Bercaw, J. E. *J. Am. Chem. Soc.* **1985**, *107*, 2670−2682. (c) Burger, B. J.; Thompson, M. E.; Cotter, W. D.; Bercaw, J. E. *J. Am. Chem. Soc.* **1990**, *112*, 1566−1577.

(2) Clot, E.; Eisenstein, O. In *Principles and Applications of Density Functional Theory in Inorganic Chemistry II*; Kaltsoyannis, N., McGrady, J. E., Eds.; Springer: Berlin; 2004; Vol. *113*, pp 1−36.

(3) (a) Green, M. L. H.; Ohare, D. *Pure Appl. Chem.* **1985**, *57*, 1897−1910. (b) Ryabov, A. D. *Chem. Rev.* **1990**, *90*, 403−424. (c) Shilov, A. E.; Shul'pin, G. B. *Chem. Rev.* **1997**, *97*, 2879−2932.

(4) (a) Scherer, W.; Herz, V.; Brück, A.; Hauf, C.; Reiner, F.; Altmannshofer, S.; Leusser, D.; Stalke, D. *Angew. Chem., Int. Ed.* **2011**, *50*, 2845−2849. (b) Brookhart, M.; Green, M. L. H.; Parkin, G. *Proc. Natl. Acad. Sci. U.S.A.* **2007**, *104*, 6908−6914. (c) Crabtree, R. H. In *The Organometallic Chemistry of the Transition Metals*, 2nd ed.; Wiley: New York, 1994; pp 53−54, 188−190.

(5) Dawoodi, Z.; Green, M. L. H.; Mtetwa, V. S. B.; Prout, K. *J. Chem. Soc., Chem. Commun.* **1982**, 802−803.

(6) (a) Nikonov, G. I. In *Advances in Organometallic Chemistry*; West, R., Hill, A. F., Stone, F. G. A., Eds.; Academic Press: New York, 2005; Vol. *53*, pp 217−309. (b) Corey, J. Y. *Chem. Rev.* **2011**, *111*, 863−1071.

(7) Tilley, T. D.; Andersen, R. A.; Zalkin, A. *Inorg. Chem.* **1984**, *23*, 2271−2276.

(8) (a) Lin, Z. In *Contemporary metal boron chemistry. I, Borylenes, boryls, borane σ-complexes, and borohydrides*; Marder, T. B., Lin, Z., Eds.; Springer: Berlin, 2008; pp 151−202. (b) Besora, M.; Lledós, A. In *Contemporary metal boron chemistry. I, Borylenes, boryls, borane σ-complexes, and borohydrides*; Marder, T. B., Lin, Z., Eds.; Springer: Berlin, 2008; Vol. *130*, pp 203−214.

(9) Eppinger, J.; Spiegler, M.; Hieringer, W.; Herrmann, W. A.; Anwander, R. *J. Am. Chem. Soc.* **2000**, *122*, 3080−3096.

(10) (a) Hartwig, J. F.; Muhoro, C. N.; He, X.; Eisenstein, O.; Bosque, R.; Maseras, F. *J. Am. Chem. Soc.* **1996**, *118*, 10936−10937. (b) Muhoro, C. N.; He, X.; Hartwig, J. F. *J. Am. Chem. Soc.* **1999**, *121*, 5033−5046. (c) Lam, W. H.; Lin, Z. *Organometallics* **2000**, *19*, 2625−2628.

(11) (a) Spence, R. E. v. H.; Parks, D. J.; Piers, W. E.; MacDonald, M.-A.; Zaworotko, M. J.; Rettig, S. J. *Angew. Chem., Int. Ed. Engl.* **1995**, *34*, 1230−1233. (b) Radius, U.; Silverio, S. J.; Hoffmann, R.; Gleiter, R. *Organometallics* **1996**, *15*, 3737−3745. (c) Spence, R. E. v. H.; Piers, W. E.; Sun, Y.; Parvez, M.; MacGillivray, L. R.; Zaworotko, M. J. *Organometallics* **1998**, *17*, 2459−2469.

(12) Hartwig, J. F. *J. Am. Chem. Soc.* **1996**, *118*, 7010−7011.

(13) Scherer, W.; Wolstenholme, D. J.; Herz, V.; Eickerling, G.; Brück, A.; Benndorf, P.; Roesky, P. W. *Angew. Chem., Int. Ed.* **2010**, *49*, 2242−2246.

(14) (a) Hanley, P. S.; Hartwig, J. F. *J. Am. Chem. Soc.* **2011**, *133*, 15661−15673. (b) Neukom, J. D.; Perch, N. S.; Wolfe, J. P. *Organometallics* **2011**, *30*, 1269−1277. (c) Hanley, P. S.; Markovic, D.; Hartwig, J. F. *J. Am. Chem. Soc.* **2010**, *132*, 6302−6303. (d) Neukom, J. D.; Perch, N. S.; Wolfe, J. P. *J. Am. Chem. Soc.* **2010**, *132*, 6276−6277.

(15) Chen, F.; Fan, S.; Wang, Y.; Chen, J.; Luo, Y. *Organometallics* **2012**, *31*, 3730−3735.

(16) Yan, K.; Ellern, A.; Sadow, A. D. *J. Am. Chem. Soc.* **2012**, *134*, 9154−9156.

(17) Yan, K.; Sadow, A. D. *Chem. Commun.* **2013**, *49*, 3212−3214.

(18) Herrmann, W. A.; Huber, N. W.; Behm, J. *Chem. Ber.* **1992**, *125*, 1405−1407.

(19) (a) Herrmann, W. A.; Eppinger, J.; Runte, O.; Spiegler, M.; Anwander, R. *Organometallics* **1997**, *16*, 1813−1815. (b) Klimpel, M. G.; Gorlitzer, H. W.; Tafipolsky, M.; Spiegler, M.; Scherer, W.; Anwander, R. *J. Organomet. Chem.* **2002**, *647*, 236−244.

(20) (a) Harris, D. H.; Lappert, M. F. In *Organometallic Chemistry Reviews: Organosilicon Reviews*; Elsevier: Amsterdam, 1976; p 13. (b) Bradley, D. C.; Chisholm, M. H. *Acc. Chem. Res.* **1976**, *9*, 273−280. (c) Ghotra, J. S.; Hursthouse, M. B.; Welch, A. J. *J. Chem. Soc., Chem. Commun.* **1973**, 669−700. (d) Andersen, R. A.; Templeton, D. H.; Zalkin, A. *Inorg. Chem.* **1978**, *17*, 2317−2319. (e) Bradley, D. C.; Ghotra, J. S.; Hart, F. A.; Hursthouse, M. B.; Raithby, P. R. *J. Chem. Soc., Chem. Commun.* **1972**, 1225−1226.

(21) Anwander, R.; Runte, O.; Eppinger, J.; Gerstberger, G.; Herdtweck, E.; Spiegler, M. *J. Chem. Soc., Dalton Trans.* **1998**, 847−858.

(22) Procopio, L. J.; Carroll, P. J.; Berry, D. H. *J. Am. Chem. Soc.* **1994**, *116*, 177−185.

(23) Herrmann, W. A.; Munck, F. C.; Artus, G. R. J.; Runte, O.; Anwander, R. *Organometallics* **1997**, *16*, 682−688.

(24) Wolfsberg, M. *Acc. Chem. Res.* **1972**, *5*, 225−233.

(25) See the Supporting Information for full characterization of $[HB(C_6F_5)_3]^-$ and $[B(C_6F_5)_4]^-$ salts.

(26) Tilley, T. D. *Organometallics* **1985**, *4*, 1452−1457.

(27) Procopio, L. J.; Carroll, P. J.; Berry, D. H. *J. Am. Chem. Soc.* **1991**, *113*, 1870−1872.

(28) (a) Pople, J. A.; Binkley, J. S.; Seeger, R. *Int. J. Quantum Chem.* **1976**, *S10*, 1−19. (b) Møller, C.; Plesset, M. S. *Phys. Rev.* **1934**, *46*, 618−622.
(29) (a) Sakai, Y.; Miyoshi, E.; Klobukowski, M.; Huzinaga, S. *J. Chem. Phys.* **1997**, *106*, 8084−8092. (b) Osanai, Y.; Soejima, E.; Noro, T.; Mori, H.; Ma San, M.; Klobukowski, M. *Chem. Phys. Lett.* **2008**, *463*, 230−234.
(30) Schmidt, M. W.; Baldridge, K. K.; Boatz, J. A.; Elbert, S. T.; Gordon, M. S.; Jensen, J. H.; Koseki, S.; Matsunaga, N.; Nguyen, K. A.; Su, S. J.; Windus, T. L.; Dupuis, M.; Montgomery, J. A. *J. Comput. Chem.* **1993**, *14*, 1347−1363.
(31) Gordon, M. S.; Schmidt, M. W. In *Theory and Applications of Computational Chemistry*; Dykstra, C. E., Frenking, G., Kim, K. S., Scuseria, G. E., Eds.; Elsevier: Amsterdam, 2005; pp 1167−1189.
(32) Edmiston, C.; Ruedenberg, K. *Rev. Mod. Phys.* **1963**, *35*, 457−465.
(33) (a) Walker, D. A.; Woodman, T. J.; Hughes, D. L.; Bochmann, M. *Organometallics* **2001**, *20*, 3772−3776. (b) Milione, S.; Grisi, F.; Centore, R.; Tuzi, A. *Organometallics* **2006**, *25*, 266−274. (c) Garner, L. E.; Zhu, H.; Hlavinka, M. L.; Hagadorn, J. R.; Chen, E. Y. X. *J. Am. Chem. Soc.* **2006**, *128*, 14822−14823.
(34) Zhu, J.; Mukherjee, D.; Sadow, A. D. *Chem. Commun.* **2012**, *48*, 464−466.
(35) Uhlig, W.; Tretner, C. *J. Organomet. Chem.* **1994**, *467*, 31−35.
(36) Luinstra, G. A.; Rief, U.; Prosenc, M. H. *Organometallics* **1995**, *14*, 1551−1552.
(37) Cordero, B.; Gómez, V.; Platero-Prats, A. E.; Revés, M.; Echeverría, J.; Cremades, E.; Barragán, F.; Alvarez, S. *Dalton Trans.* **2008**, 2832−2838.
(38) Chaudhry, S. C.; Kummer, D. *J. Organomet. Chem.* **1988**, *339*, 241−252.
(39) Passarelli, V.; Zanella, P. *Eur. J. Inorg. Chem.* **2004**, 4439−4446.
(40) Forster, T. D.; Tuononen, H. M.; Parvez, M.; Roesler, R. *J. Am. Chem. Soc.* **2009**, *131*, 6689−6691.
(41) Simpson, S. J.; Andersen, R. A. *Inorg. Chem.* **1981**, *20*, 3627−3629.
(42) Green, M. L. H. *J. Organomet. Chem.* **1995**, *500*, 127−148.
(43) Male, N. A. H.; Thornton-Pett, M.; Bochmann, M. *J. Chem. Soc., Dalton Trans.* **1997**, 2487−2494.
(44) Enders, M.; Fink, J.; Maillant, V.; Pritzkow, H. *Z. Anorg. Allg. Chem.* **2001**, *627*, 2281−2288.
(45) Kidd, R. G. In *Boron-11 in NMR of Newly Accessible Nuclei*; Laszlo, P., Ed.; Academic Press: New York, 1983; Vol. *2*, Chapter 3.
(46) (a) Lambert, J. B.; Kania, L.; Zhang, S. *Chem. Rev.* **1995**, *95*, 1191−1201. (b) Reed, C. A. *Acc. Chem. Res.* **1998**, *31*, 325−332. (c) Scott, V. J.; Celenligil-Cetin, R.; Ozerov, O. V. *J. Am. Chem. Soc.* **2005**, *127*, 2852−2853. (d) Reed, C. A. *Acc. Chem. Res.* **2009**, *43*, 121−128.
(47) (a) Parks, D. J.; Blackwell, J. M.; Piers, W. E. *J. Org. Chem.* **2000**, *65*, 3090−3098. (b) Gevorgyan, V.; Rubin, M.; Benson, S.; Liu, J.-X.; Yamamoto, Y. *J. Org. Chem.* **2000**, *65*, 6179−6186. (c) Rubin, M.; Schwier, T.; Gevorgyan, V. *J. Org. Chem.* **2002**, *67*, 1936−1940.
(48) (a) Müller, T. *Angew. Chem., Int. Ed.* **2001**, *40*, 3033−3036. (b) Panisch, R.; Bolte, M.; Müller, T. *J. Am. Chem. Soc.* **2006**, *128*, 9676−9682. (c) Hoffmann, S. P.; Kato, T.; Tham, F. S.; Reed, C. A. *Chem. Commun.* **2006**, 767−769.
(49) Yan, K.; Upton, B. M.; Ellern, A.; Sadow, A. D. *J. Am. Chem. Soc.* **2009**, *131*, 15110−15111.
(50) (a) Collman, J. P.; Hegedus, L. S. In *Principles and Applications of Organotransition Metal Chemistry*; Kelly, A., Ed.; University Science Books: Sausalito, CA, 1980. (b) Calderazzo, F. *Angew. Chem., Int. Ed. Engl.* **1977**, *16*, 299−311. (c) Berke, H.; Hoffman, R. *J. Am. Chem. Soc.* **1978**, *100*, 7224−7236.
(51) Brintzinger, H. H.; Fischer, D.; Mülhaupt, R.; Rieger, B.; Waymouth, R. M. *Angew. Chem., Int. Ed. Engl.* **1995**, *34*, 1143−1170.
(52) Evans, W. J.; Perotti, J. M.; Ziller, J. W. *Inorg. Chem.* **2005**, *44*, 5820−5825.
(53) Baudry, D.; Dormond, A.; Lachot, B.; Visseaux, M.; Zucchi, G. *J. Organomet. Chem.* **1997**, *547*, 157−165.
(54) Werkema, E. L.; Andersen, R. A.; Yahia, A.; Maron, L.; Eisenstein, O. *Organometallics* **2009**, *28*, 3173−3185.
(55) Liu, F.-C.; Liu, J.; Meyers, E. A.; Shore, S. G. *Inorg. Chem.* **1999**, *38*, 2169−2173.
(56) Yan, K.; Schoendorff, G.; Upton, B. M.; Ellern, A.; Windus, T. L.; Sadow, A. D. *Organometallics* **2013**, *32*, 1300−1316.
(57) Harvey, M. J.; Hanusa, T. P.; Pink, M. *Chem. Commun.* **2000**, 489−490.
(58) Holton, J.; Lappert, M. F.; Ballard, D. G. H.; Pearce, R.; Atwood, J. L.; Hunter, W. E. *J. Chem. Soc., Dalton Trans.* **1979**, 54−61.
(59) (a) Watson, P, L.; Herskovitz, T. In *Initiation of Polymerization*; Bailey, F. E., Vandenberg, E. J., Blumstein, A., Bowden, M. J., Arthur, J. C., Lal, J., Ottenbrite, R. M., Eds.; American Chemical Society: Washington, DC, 1983; ACS Symposium Series *212*, pp 459−479. (b) Watson, P. L.; Parshall, G. W. *Acc. Chem. Res.* **1985**, *18*, 51−56.
(60) Bochmann, M.; Lancaster, S. J. *Angew. Chem., Int. Ed.* **1994**, *33*, 1634−1637.
(61) Klimpel, M. G.; Sirsch, P.; Scherer, W.; Anwander, R. *Angew. Chem., Int. Ed.* **2003**, *42*, 574−577.
(62) Corriu, R. J. P.; Perz, R.; Réye, C. *Tetrahedron* **1983**, *39*, 999−1009.
(63) Stockland, R. A., Jr.; Jordan, R. F. *J. Am. Chem. Soc.* **2000**, *122*, 6315−6316.
(64) Burger, B. J. Ph.D. Thesis, California Institute of Technology, 1987.
(65) Parks, D. J.; Piers, W. E. *J. Am. Chem. Soc.* **1996**, *118*, 9440−9441.
(66) Shirobokov, O. G.; Kuzmina, L. G.; Nikonov, G. I. *J. Am. Chem. Soc.* **2011**, *133*, 6487−6489.
(67) (a) Du, G.; Abu-Omar, M. M. *Organometallics* **2006**, *25*, 4920−4923. (b) Du, G.; Fanwick, P. E.; Abu-Omar, M. M. *J. Am. Chem. Soc.* **2007**, *129*, 5180−5187.
(68) (a) Yang, J.; White, P. S.; Schauer, C. K.; Brookhart, M. *Angew. Chem., Int. Ed.* **2008**, *47*, 4141−4143. (b) Park, S.; Brookhart, M. *Organometallics* **2010**, *29*, 6057−6064.